



Molecular basis for thiocarboxylation and release of Urm1 by its E1-activating enzyme Uba4

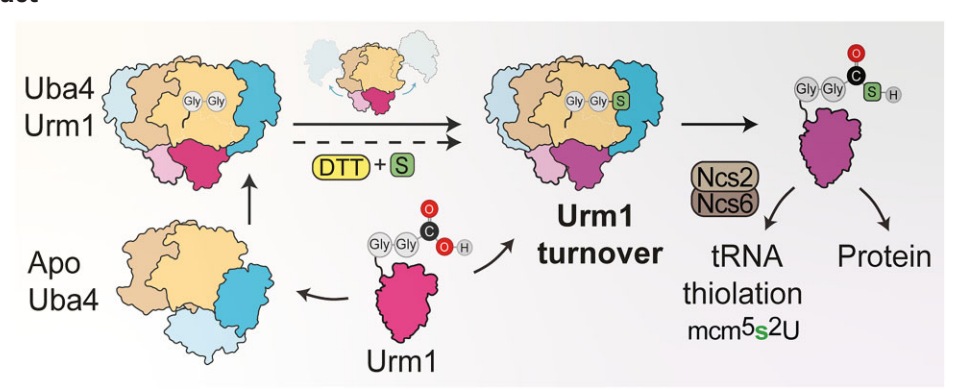
Mikołaj Sokołowski^{1,2,†}, Dominika Kwasna^{1,†}, Keerthiraju E. Ravichandran^{1,2}, Cristian Eggers³, Rościsław Krutyhołowa¹, Magdalena Kaczmarczyk¹, Bozena Skupien-Rabian¹, Marcin Jaciuk¹, Marta Walczak^{1,4}, Priyanka Dahate^{1,4}, Marta Pabis¹, Małgorzata Jemioła-Rzemińska⁵, Urszula Jankowska¹, Sebastian A. Leidel ^{©3} and Sebastian Glatt ^{©1,6,*}

Present address: Rościsław Krutyhołowa, ETH Zürich, Institute of Molecular Biology and Biophysics, Zurich, Switzerland.

Abstract

Ubiquitin-related modifier 1 (Urm1) is a highly conserved member of the ubiquitin-like (UBL) family of proteins. Urm1 is a key component of the eukaryotic transfer RNA (tRNA) thiolation cascade, responsible for introducing sulfur at wobble uridine (U₃₄) in several eukaryotic tRNAs. Urm1 must be thiocarboxylated (Urm1-SH) by its E1 activating enzyme UBL protein activator 4 (Uba4). Uba4 first adenylates and then thiocarboxylates the C-terminus of Urm1 using its adenyl-transferase (AD) and rhodanese (RHD) domains. However, the detailed mechanisms of Uba4, the interplay between the two domains, and the release of Urm1 remain elusive. Here, we report a cryo-EM-based structural model of the Uba4/Urm1 complex that reveals the position of its RHD domains after Urm1 binding, and by analyzing the in vitro and in vivo consequence of mutations at the interface, we show its importance for the thiocarboxylation of Urm1. Our results confirm that the formation of the Uba4-Urm1 thioester and thiocarboxylation of Urm1's C-terminus depend on conserved cysteine residues of Uba4 and that the complex avoids unwanted side-reactions of the adenylate by forming a thioester intermediate. We show how the Urm1-SH product can be released and how Urm1 interacts with upstream (Tum1) and downstream (Ncs6) components of the pathway. Our work provides a detailed mechanistic description of the reaction steps that are needed to produce Urm1-SH, which is required to thiolate tRNAs and persulfidate proteins.

Graphical abstract



Introduction

Thiolation of wobble uridine (U₃₄) in transfer RNAs (tR-NAs) is a universally conserved posttranscriptional RNA

modification that plays a pivotal role in translational fidelity, reading-frame maintenance, translation-elongation rates and co-translational folding dynamics (1-4). Changes in tRNA

(https://creativecommons.org/licenses/by-nc/4.0/), which permits non-commercial re-use, distribution, and reproduction in any medium, provided the original work is properly cited. For commercial re-use, please contact reprints@oup.com for reprints and translation rights for reprints. All other permissions can be obtained through our RightsLink service via the Permissions link on the article page on our site—for further information please contact journals.permissions@oup.com.

¹Malopolska Centre of Biotechnology (MCB), Jagiellonian University, Gronostajowa7a, 30-387 Krakow, Poland

²Postgraduate School of Molecular Medicine, Zwirki i Wigury 61, 02-091 Warsaw, Poland

³Department of Chemistry, Biochemistry and Pharmaceutical Sciences, University of Bern, Freiestrasse 3, 3012 Bern, Switzerland

⁴Doctoral School of Exact and Natural Sciences, Jagiellonian University, prof. S. Łojasiewicza 11, 30-348 Krakow, Poland

⁵Faculty of Biochemistry, Biophysics and Biotechnology, Jagiellonian University, Gronostajowa 7, 30-387 Krakow, Poland

⁶Department for Biological Sciences and Pathobiology, University of Veterinary Medicine Vienna, Veterinaerplatz 1, 1210 Vienna, Austria

^{*}To whom correspondence should be addressed. Tel: +48 012 664 6321; Email: sebastian.glatt@ui.edu.pl

[†]The first two authors should be regarded as Joint First Authors.

thiolation levels have been implicated in the cellular response to changing environmental conditions and in the regulation of sulfur, carbon, and nitrogen metabolic homeostasis (5–7). Two distinct enzyme families catalyze s²U₃₄-tRNA formation in bacteria/mitochondria (i.e. MnmA-like) and in archaea/eukaryotes (Ncs6/CTU1-like), respectively (8,9).

The ubiquitin-related modifier 1 (Urm1) pathway is responsible for the 2-thiolation of U₃₄ in three cytoplasmic tRNAs, $tRNA_{UUU}^{Lys}$, $tRNA_{UUC}^{Glu}$, $tRNA_{UUG}^{Gln}$ in all eukaryotes, and additionally tRNA_{UCU} in vertebrates (10). The components of the canonical Urm1 pathway have been described (10-12) and comprise a series of sulfur transfer enzymes that relay sulfur from L-cysteine to the sulfur-transferase complex. The transferase complex (Ncs2/Ncs6 in yeast and CTU1/CTU2 in humans) binds Urm1, selectively recruits target tRNAs and thiolates them (Figure 1A). Urm1 was originally identified during the search for unknown ubiquitin-like proteins (UBLs) in yeast (13), and like other UBLs, can be covalently conjugated to target proteins (14–16). Recently, it was shown that thiocarboxylated Urm1 covalently attaches to target proteins in vitro without the need for E2/E3-like enzymes (17). Strikingly, the conjugation activity of Urm1 depends on the presence of the thiocarboxylate group at the C-terminus, the sulfur of which is transferred to selected cysteine residues in the target proteins during the conjugation reaction. Hence, the Urm1 pathway can not only relay sulfur to tRNAs but also to specific proteins, which results in cysteine persulfidation that represents a novel targeted protection mechanism against oxidative stress

Urm1 and its E1-activating enzyme Uba4 (MOCS3 in humans) share similarities with prokaryotic sulfur-carrier protein (SCP) cascades as well as with the eukaryotic UBL conjugation systems (18). Consequently, the pathway is thought to represent a molecular fossil that stands at the evolutionary branch point between SCPs and E1-UBL systems found in present-day eukaryotes (19,20). Like all other SCPs and E1 activating enzymes (21), Uba4 first adenylates the C-terminus of Urm1 by hydrolyzing an ATP molecule in its adenyltransferase domain (AD). Subsequently, a thioester-mediated intermediate is formed between the C-terminal glycine of Urm1 and a strictly conserved cysteine residue of Uba4 (22). In contrast to the canonical E1-UBL cascades, Urm1 is further thiocarboxylated by the C-terminal rhodanese domain (RHD) of Uba4, which has received a persulfide from Nfs1 (and/or Tum1) (23) (Figure 1A). This reaction is similar to the bacterial MoaD-MoeB and ThiS-ThiF systems, which are responsible for delivering sulfur for the synthesis of molybdopterin cofactor (moco) and thiamin (also known as vitamin B_1) (24,25). MoaD receives the sulfur atom directly from a cysteine desulfurase (26), whereas in the case of the ThiS-ThiF complex, sulfur is delivered by the TusA protein (27). In contrast to archaeal SCPs that use separate RHD proteins to deliver the necessary persulfide (28–30), Uba4 contains an integrated RHD domain at its C-terminus (31). The domain is directly fused to the AD via a flexible linker region, and it is critical for the thiocarboxylation step and the final release of Urm1 from the Uba4-Urm1 complex. The crystal structures of CtUba4 purified from the thermophilic fungus Chaetomium thermophilum (Ct), also known as Thermochaetoides thermophila provided the first structural insights into eukaryotic Uba4 proteins, showing that the two RHD domains dimerize and asymmetrically localize to one side of the homodimer

of ADs (31). The crystal structure of the *Ct*Uba4_{C202K}-Urm1 complex demonstrated how the C-terminus of Urm1 enters the catalytic center of the AD and that binding of Urm1 apparently dissolves and displaces the dimer of RHD domains. Strikingly, the RHD domains of Uba4 become flexible and are not visible in the electron density maps of Uba4 bound to Urm1. Hence, the mechanistic details of how the two RHD domains and their catalytic cysteines are positioned during the thiocarboxylation step remain elusive.

Here, we report structures of the Uba4-Urm1 complex by single particle cryo-electron microscopy (cryo-EM) at an overall resolution of up to 5.9 Å. The observed states not only confirm previous intermediates, but also reveal the position of the RHD domains of Uba4 in close proximity to the catalytic site of the AD. Complementary mutational and biochemical analyses show the precise requirements for binding, adenylation, acyl-disulfide formation, thiocarboxylation and release of Urm1 from Uba4. Hence, our results show that Urm1 stays in place during adenylation and thioester formation like in other E1s. Moreover, the RHD domains of Uba4 undergo relative rearrangements around the stably bound AD-Urm1 module to conduct the final reaction step. Furthermore, we show how the complex achieves substrate specificity and avoids off-target effects. Finally, we characterize the specific interplay between Urm1 and its upstream (Tum1) and downstream (Ncs2/Ncs6) partners in the thiolation cascade. Our work provides mechanistic insights into the key steps that lead to the thiocarboxylation of Urm1, which further corroborate that the Urm1 system represents an evolutionary link between bacterial SCP and eukaryotic UBL systems.

Materials and methods

Protein expression

Genes encoding the ORFs for the proteins of interest were cloned into pETM30 or pETM11 vectors harboring GST-Histag or His-tag at the N terminus respectively. *Escherichia coli* pRARE strain cell were transformed with an expression vector and selected against Kanamycin. Bacterial cultures were inoculated in a 100 ml LB-broth overnight pre-culture, with shaking at 250 rpm at 37°C. The next day, the pre-culture was used to inoculate 1 L cultures (1/100 dilution). The cultures were grown at 37°C shaking at 180 rpm, until reaching an OD600 of 0.5–0.6. The cultures were then induced with 0.5 mM Isopropyl β - d-1-thiogalactopyranoside (IPTG) and grown overnight at 18°C, while shaking. The next day, the cultures were harvested by centrifugation (10 min at 8000 \times g) and the resulting bacterial pellets were used immediately for protein purification or stored at -80° C until further use.

Purification of Uba4 and Urm1 and Tum1 constructs

The bacterial pellets were resuspended in lysis buffer (30 mM HEPES, pH 8.0, 300 mM NaCl, 20 mM imidazole, 0.15% Triton X-100, 10 mM MgSO₄, 1 mM β -mercaptoethanol, 10 mg/ml DNase, 1 mg/ml lysozyme, 10% glycerol, cocktail of protease inhibitors) and lysed using a high-pressure homogenizer Emulsiflex C3 (Avestin). The homogenized lysates were then centrifuged at 60 000 × g for 1 h at 4°C. The supernatants were used in either Ni-NTA-based affinity purification with Ni-NTA agarose (Qiagen) using gravity-flow columns (Thermo Fischer Scientific), or GST-based affinity

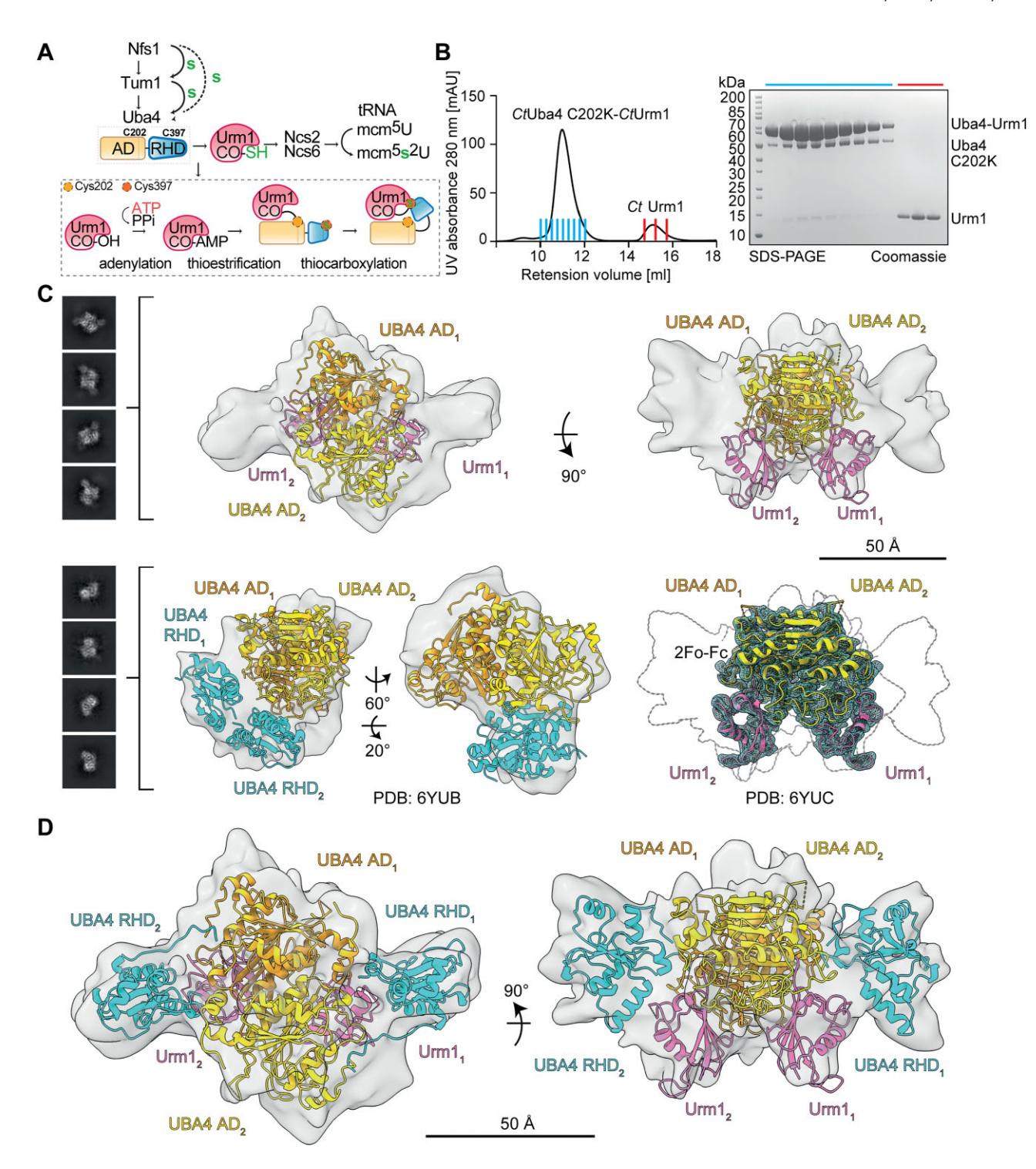


Figure 1. RHD domains of Uba4 are displaced upon Urm1 binding and can move close to the Urm1 C-terminus. (**A**) The eukaryotic thiolation cascade involves the relay of activated sulfur from Nfs1 via Tum1 to Uba4, where it becomes a persulfide on the catalytic cysteine (Cys397) of the RHD domain. Uba4 binds Urm1 via its AD, adenylates the C-terminus of Urm1 and subsequently forms a thioester intermediate with a conserved cysteine (Cys202 in CtUba4). An intramolecular protein transfer allows the persulfided RHD domain to thiocarboxylate the C-terminus of Urm1. Ultimately, thiocarboxylated Urm1 delivers the sulfur atom to the Ncs2/Ncs6 complex, which binds specific tRNAs and carries out the final tRNA thiolation reaction. (**B**) Gel filtration profile and SDS-PAGE analyses of the purified CtUba4c_{202K}-CtUrm1 complex. Of note, the complex is formed via an iso-peptide bond between the introduced Lys202 residue of CtUba4 and the C-terminal glycine of CtUrm1, which is confirmed by a shift on the denaturing SDS-PAGE gel. (**C**) Representative 2D classes obtained from the cryo-EM dataset. After subsequent *ab initio* analyses, we identified two classes: one class fitted the CtUba4c_{202K}-CtUrm1 complex (PDB ID: 6Z6S) but displayed additional wing-like densities on each side of the complex (top) and one resembling the previously determined crystal structure of CtUba4c_{202K} (bottom left, PDB ID: 6YUB). These additional densities were not visible in the electron density maps (2Fc-Fo) of the previously determined crystal structure of the CtUba4c_{202K}-CtUrm1 complex (bottom right, PDB ID: 6YUC). ADs (yellow/orange), RHD domains (cyan) and Urm1 (pink) are colored and labeled. Scale bar for 50 Å is shown. (**D**) Model of the CtUba4c_{202K}/Urm1 complex after molecular dynamic flexible fitting of the two RHD domains into the additional densities. RHD domains are located at the sides, with each of the catalytic cysteines positioned towards the C-terminus of Urm1. Scale bar for 50 Å is shown.

purification with GSTrap column (Cytiva) on a FPLC system (ÄKTAstart; Cytiva) according to the manufacturer's protocols. In case of Ni-NTA-based purification protocol, buffers were supplemented with 20 mM imidazole. Proteins were eluted from the affinity-resin by either NiNTA-elution buffer (30 mM HEPES pH 8.0, 300 mM NaCl, 250 mM imidazole, 0.15% Triton X-100, 1 mM β-mercaptoethanol, 10% glycerol) or GST-elution buffer (30 mM HEPES, pH 8.0, 300 mM NaCl, 10 mM reduced glutathione, 0.15% Triton X-100, 1 mM β-mercaptoethanol, 10% glycerol), respectively. After elution, the protein was dialyzed overnight against dialysis buffer (30 mM HEPES, pH 8.0, 300 mM NaCl, 20 mM imidazole [in case of NiNTA elution], 1 mM β-mercaptoethanol, 10% glycerol), using Slide-A-Lyzer dialysis cassettes (Thermo Fischer Scientific). N-terminal affinity tags were optionally cleaved at this stage by adding a 6xHisor GST-tagged TEV protease during dialysis. The cleaved tag, as well as the TEV protease, were subsequently removed in a second Ni-NTA/GST affinity chromatography step. Finally, proteins were loaded on either HiLoad 26/600 Superdex 200 (Cytiva) or HiLoad 16/600 Superdex 75 (Cytiva) for Uba4 and Urm1, respectively. Purified and concentrated proteins were stored at -80° C in storage buffer (20 mM HEPES, pH 8.0, 150 mM NaCl, 1 mM Dithiothreitol (DTT)) for further usage.

Purification of Ncs2 and Ncs6 constructs

Bacterial pellets were resuspended in Ncs-lysis buffer (50 mM Tris-HCl, pH 8.0, 300 mM NaCl, 0.15% Triton X-100, 10 mM MgSO₄, 1 mM DTT, 10 mg/ml DNase, 1 mg/ml lysozyme, 10% glycerol, cocktail of protease inhibitors) and lysed using a high-pressure homogenizer Emulsiflex C3 (Avestin). To form the CtNcs2/6 complex, pellets containing each construct were mixed with each other before lysis. The proteins were purified with GST HiTrap (Cytiva) columns on a ÄKTAstart system (Cytiva) using standard conditions. Elution was achieved by applying Ncs-GST elution buffer (50 mM Tris-HCl, pH 8.0, 300 mM NaCl, 1 mM MgCl₂, 10 mM reduced glutathione, 1 mM DTT). After elution from the GSTrap column, the proteins were dialyzed overnight into Ncs-dialysis buffer (50 mM Tris-HCl, pH 8.0, 300 mM NaCl, 1 mM DTT), using Slide-A-Lyzer dialysis cassettes (Thermo Fischer Scientific). Tags were optionally cleaved with GST-tagged TEV protease and removed with a second GSTrap affinity chromatography step. Finally, the proteins were purified by size-exclusion chromatography (SEC) on a HiLoad 26/600 Superdex 200 prep grade column (Cytiva) using a ÄKTAstart system. Purified and concentrated proteins were stored at -80° C in Ncs-storage buffer (20 mM Tris-HCl, pH 8.0, 150 mM NaCl, 1 mM DTT).

SEC-based protein interaction

Uba4-Urm1 complex formation was assessed using a Superdex 200 Increase 10/300 GL column (Cytiva) on a ÄK-TApure system. For a standard 1:1 molar ratio of the Uba4 and Urm1 subunits, 20 μM of each was incubated in 400 μl of storage buffer (without DTT) for 1 h at 30°C (Saccharomyces cerevisiae) or 37°C (C. thermophilum). Fractions from the separation were analyzed on denaturing sodium dodecyl sulfate-polyacrylamide gel electrophoresis (SDS-PAGE) gels and visualized using Coomassie stain.

Isothermal titration calorimetry (ITC)

The interaction of Ncs2 and Ncs6 proteins was quantified at 4°C using a Nano ITC 2G device (TA instruments), according to the manufacturer's protocol. Protein samples were thoroughly dialyzed into Ncs-dialysis buffer and degassed before use. Approximately 80 μM of Ncs2 was loaded into the syringe and 8 μM of Ncs6 was placed in the sample cell. Each injection (7 μ l) was performed in 300 s intervals. Experiments were conducted at 25°C with a stirring rate of 250 rpm. To account for the heat of dilution, control experiments were completed by titrating Ncs2 protein into a buffer. Integrated areas under each injection peak were plotted against the molar ratio of the injected Ncs2. An independent binding model was fitted to the data using the manufacturer's software to determine the estimated $K_{\rm d}$ of the interaction. The experiment was performed in three independent technical repeats.

GST-pulldown assay for protein interaction

Untagged proteins of interest were incubated with a putative binding partners tagged with a GST-tag. For CtUba4-GST-CtUrm1 assays, the storage buffer was used, and the Ncsstorage buffer was used for assays involving either Ncs2, Ncs6 or Ncs2/Ncs6. Samples were prepared in a total volume of 500 μl, with individual protein concentrations between 1 and 2 μM. ATP or DTT were added at a final concentration of 1 mM. The sample was added to equilibrated Glutathione Sepharose 4B beads (GE Healthcare) and incubated on a rotating wheel for 120 min at 4°C. After binding, glutathione beads were collected by gentle spinning $(500 \times g)$ and subsequently washed three times with the storage buffer containing 0.05% (v/v) Tween 20. Bound proteins were denatured at 95°C in the presence of Laemmli sample buffer and analyzed on BoltTM 4–12% Bis-Tris Plus Gels (Thermo Fisher Scientific). The gels were stained with Coomassie Brilliant Blue for visualization. Inputs were collected after the reaction and before the pulldown, representing \sim 5% of the complete reaction.

CtUba4-Urm1 conjugation assay

Conjugation of *Ct*Uba4_{C202K} to Urm1 was done as described previously (31). In detail, freshly purified *Ct*Uba4_{C202K} and *Ct*Urm1 were incubated together with ATP at 1:1.25:2.25 molar ratios in conjugation buffer (100 mM 2-(N-morpholino)ethanesulfonic acid (MES), pH 6.0, 100 mM NaCl, 2 mM MgCl₂) at 37°C for 1 h and loaded on Superdex 200 Increase 10/300 GL column (Cytiva) on an ÄKTApure system. Fractions were analyzed by SDS-PAGE for purity and stoichiometry and selected for subsequent cryo-EM sample preparation.

Cryo-EM sample preparation

Freshly purified CtUba4 $_{C202K}$ and CtUrm1 were mixed at 1:1 molar ratio to reach final 0.3 mg/ml concentration of the sample. Approximately 2.5 μ l of the sample was next applied on glow-discharged (8 mA, 60 s) Quantifoil R2/1 200 mesh copper grids, and vitrifed in a ThermoFisher Mark IV Vitrobot set to 4°C and 100% air humidity, with 15 s sample incubation, blot force 5 and blot time 5 s. Grids screening and the data collection was carried out at the SOLARIS National Synchrotron Radiation Centre UJ, Kraków, Poland.

Cryo-EM data analyses and structure determination

In total 5150 micrographs were collected on a ThermoFisher Titan Krios G3i microscope operating at a 300 kV acceleration voltage equipped with K3 direct electron detector and energy filter. Data preprocessing was done in WARP (32) while the full analysis was carried in cryoSPARC software.

Alphafold prediction of Uba4-Urm1 heterotetramers

AlphaFold models of Uba4-Urm1 complexes were generated using alphafold-multimer incorporated into a colabfold jupyter notebook. Colabfold operated in the unpaired mode, using the mmseqs2 MSA method, and the number of recycles equal to 3. Input sequences encoding *S. cerevisiae*, *C. thermophilum* and *Homo sapiens* Uba4 and Urm1 orthologs were obtained from Uniprot database (corresponding IDs P38820, P40554, G0SC54, G0SE11, O95396, Q9BTM9) and used as input in 2:2 stoichiometry for modeling. For every organism, five models were generated. *Sc*Uba4-Urm1 AlphaFold2 model was colored by its conservation grade generated with ConSurf server (33). Multiple Sequence Alignment was built with CLUSTALW and the homology level was calculated with the HMMER search algorithm.

Thioester formation assays

Thioester formation between CtUba4 and CtUrm1 was measured over time in thioester buffer (20 mM HEPES pH 7.5, 150 mM NaCl, 2 mM MgCl₂). All proteins used in the assay were first desalted using PD-SpinTrap G25 (Sigma) desalting columns, to efficiently remove reductants present in the protein storage buffers. Approximately 10 µM of CtUba4 was mixed with 20 µM of CtUrm1 prior to ATP addition to final 10 μM concentration. The reaction was incubated at 30°C and stopped by denaturation at 95°C in presence of Laemmli sample buffer. Of note, the Laemmli sample buffer did not contain reducing agents that could cleave the thioester bond. Next, 12% Bis-Tris Plus Gels (Thermo Fisher Scientific) gels were used to analyze thioester formation, limiting extraneous oxidation. Thioester formation between CtUba4 and CtUrm1 was measured in the context of varying ATP concentrations. Approximately 10 μM of CtUba4 was mixed with 20 μM of CtUrm1 in the thioester buffer and incubated at 37°C. ATP was added at a range of 1–1000 μM and the reactions were incubated for 30 min. Samples were then prepared as described for the for samples from *S. cerevisiae* (see above).

Spotting assay

Exponentially growing yeast cultures were adjusted to $OD_{600} = 0.4$, and a 1:5 serial dilution was spotted on YPD plates supplemented with rapamycin at 1, 3 or 10 nM. The plates were incubated at 30°C or 37°C for 3 days. Images were taken at days 2 and 3.

Northern blot for tRNA thiolation

Five OD_{600} of yeast were pelleted by centrifugation, resuspended in 400 μ l lysis buffer (50 mM NaOAc, pH 5.5, 10 mM EDTA pH 8.0, 1% SDS) and lysed using a bead-beater. The cell lysate was cleared by centrifugation and total RNA was extracted with acidic phenol/chloroform. Approximately 1 μ g of total RNA was separated on a 10% denaturing polyacrylamide gel (8 M urea, 0.5% TBE). The RNA was trans-

ferred to a Nylon membrane (Immobilon-Ny+) in 0.5x TBE buffer at 400 mA for 45 min. To analyze the thiolation levels of tRNA_{UUC}, the gel was supplemented with 60 μg/ml ([*N*-acryloyloyloplementy])mercuric chloride (APM). The transfer of tRNA to the nylon membrane was performed at 400 mA for 1 h; 0.5x TBE buffer was supplemented with 10 mM DTT. Northern blotting was perform as described previously (10) with minor changes. Briefly, the membrane was crosslinked with UV light (0.120 J) and hybridized at 42°C using a ³²P-5 labeled DNA probe complementary to a 3 segment of tRNA_{UUC} (5′-tggctccgatacggggagtcgaac-3′).

In vitro thiocarboxylation assays

All proteins used in thiocarboxylation assays were first desalted with PD-SpinTrap G25 (Sigma) columns and equilibrated into the thiocarboxylation buffer (20 mM HEPES, pH 8.5, 150 mM NaCl, 2 mM MgCl₂, 1 mM Tris(2carboxyethyl)phosphine (TCEP)). Reactions were incubated for 30 min at 30°C for S. cerevisiae proteins and at 37°C for C. thermophilum proteins. Default protein concentrations were as follows: 10 µM for Uba4 and 20 µM for Urm1. ATP and Na₂SSO₃ were added to a final concentration of 5 mM. After incubation, the reactions were desalted twice, to ensure the complete removal of ATP and the respective sulfur source. Samples were denatured at 95°C in Laemmli sample buffer (without DTT), supplemented with 1 mM TCEP and 1 mM EDTA. Subsequently, samples were run on SDS-PAGE gels containing 200 µM APM. All samples were also analyzed on 12% Bis-Tris Plus Gels (Thermo Fisher Scientific) to serve as loading controls. For thiocarboxylation without reducing agent, TCEP was omitted from the thiocarboxylation buffer. DTT-driven rescue of inactive cysteine mutants was assessed by thiocarboxylation of ScUrm1 by ScUba4C225A and ScUba4C397A in the absence of any reducing agent and a titration of 0-1 mM DTT. Thiocarboxylation using different sulfur sources was performed for S. cerevisiae proteins as described above, using 5 mM of either Na₂SSO₃, β-Mercaptopyruvate or L-cysteine as sulfur source.

SEC-coupled thiocarboxylation assays

To assess release of ScUrm1 from the ScUba4-ScUrm1 complex in the presence of reducing agents, thiocarboxylation reactions were followed by SEC using Superdex 200 Increase 10/300 GL column (Cytiva) on an ÄKTApure system. Reactions at different ratios were incubated in 400 µl at 30°C, and subsequently samples were immediately injected onto the column. Following the separation, fractions for ScUba4-ScUrm1 and ScUrm1 were either pooled or run separately on SDS-PAGE gels supplemented with APM and 12% Bis-Tris Plus Gels. Stimulation of ScUrm1-SH release from the ScUba4-ScUrm1 complex was analyzed by first incubating 40 µM of Uba4 with 20 μM of Urm1 and 5 mM of ATP and Na₂SSO₃ in 800 µl of thiocarboxylation buffer without TCEP. After 30 min, half of the sample was loaded directly onto the column. The second half of the sample was desalted twice before 80 uM of fresh ScUrm1 was added and incubated for another 30 min at 30°C. The sample was then immediately injected onto the column. Samples from both runs were compared on APM and 12% Bis-Tris Plus Gels, by pooling the ScUba4-ScUrm1 and free-ScUrm1 fractions.

Rescue of thiocarboxylation by Tum1

For these assays ScUba4 $_{\rm C397A}$ and ScUba4 $_{\rm C225A-C311A-C397A}$ constructs were used and ScUba4 $_{\rm WT}$ served as a positive control. Approximately 10 μ M of ScUba4 and ScTum1 were used, together with 20 μ M of ScUrm1. ScTum1 was added to the reaction mixture before the incubation at 30°C, whereas ScTum1 $_{\rm C259S}$ was used as a negative control.

SEC-coupled DTT-adduct formation

CtUrm1-DTT adduct formation was assessed by incubation of 40 μM of CtUba4 $_{\rm WT}$ or CtUba4 $_{\rm C202A}$ mutant with 40 μM of CtUrm1 in 400 μl of thioester buffer in the presence of 45 μM ATP. Approximately 1 mM DTT was added as designated. All samples were incubated for 30 min at 37°C, and then immediately injected onto the Superdex 200 Increase 10/300 GL column (Cytiva) on an ÄKTApure system. Fractions were collected as designated, and run on 12% Bis-Tris Plus Gels, excised and analyzed by mass spectrometry.

Mass spectrometry analysis

Adduct formation on the C-terminus of ScUrm1 or CtUrm1 was analyzed using micrOTOF-Q II mass spectrometer (Bruker Daltonics, Bremen, Germany) equipped with an electrospray ionization source. The instrument was calibrated just prior to measurements using ESI-L Low Concentration Tuning Mix (Agilent Technologies), and the enhanced quadratic mode was applied for the calibration curve. Samples containing ~30 μg of proteins were desalted on Amicon Ultra-0.5 Centrifugal Filter 3kDa (Millipore) using 0.05% formic acid (FA) as a washing solution. Desalted samples were mixed in 1:1 (v/v) ratio with 50% acetonitrile in 0.05% FA and directly infused to mass spectrometer with a syringe pump (KD Scientific Inc., Holliston, MA, USA) at a flow rate of 6 µl/min. Mass spectrometer was operated in positive mode with source parameters set as follows: capillary: 4.5 kV; nebulizer pressure 0.4 bar; dry gas flow 4 l/min; dry gas temperature 180°C. Nitrogen was used both as a nebulizer gas and a drying gas. The ion transfer time and pre-pulse storage time were set to 120 us and 10 us, respectively. MS scans were acquired over a m/zrange of 50-3000 using Bruker Daltonics micrOTOFcontrol software. Obtained MS spectra were deconvoluted with Maximum Entropy Deconvolution algorithm in Data Analysis 4.1 software (Bruker Daltonics, Bremen, Germany).

Electrophoretic mobility shift assay (EMSA)

The tRNA_{UUG} was *in vitro* transcribed according to previously established protocol (34). Proteins were serially diluted in electrophoretic mobility shift assay (EMSA) buffer (20 mM Tris–HCl, pH 8.0, 50 mM NaCl, 1 mM DTT), followed by the addition of Cy5-labelled tRNA_{UUG}. After incubation at 37°C for 30 min, the reactions were loaded on a 6% native gel. The gel was visualized with a fluorescence scanner (BioRad, Hercules, USA) at 670 nm. Protein inputs were checked on a denaturing SDS-PAGE and visualized by Coomassie staining.

Results

Localization of the RHD domains in the Uba4-Urm1 complex by single particle cryo-EM

Previous analyses of the Uba4-Urm1 complex have not clarified the molecular basis of the complete Uba4-Urm1 reaction

cycle. Therefore, we sought to determine the different conformations of the CtUba4-CtUrm1 complex by single particle cryo-EM to analyze and compare it to the available crystal structures. Foremost, we aimed to visualize Uba4's RHD domains after Urm1 binding, which have remained enigmatic. First, we produced and purified the CtUba4_{C202K}-CtUrm1 complex according to the previously established protocol (31) (Figure 1B), vitrified the sample, screened the grids, went through several rounds of optimization and collected a cryo-EM dataset on a Titan Krios G3i microscope (Figure 1C and Supplementary Figure S1A). Following 2D and 3D classification, we identified a certain degree of heterogeneity in the dataset, and we separated different sets of particles present in the dataset. Despite the limited resolution (Supplementary Figure S1B), the previous crystal structures of apo CtUba4 and the CtUba4C202K-CtUrm1 complex fitted well into the cryo-EM density maps corresponding to two classes of particles (Figure 1C). Strikingly, we managed to identify a class of particles that in addition to the core structure of the Uba4_{C202K}-Urm1 complex displayed two additional 'wing-shaped' densities at each side of the AD. Of note, the nominal overall resolution for this reconstruction at $GSFSC_{0.143}$ is 5.9 Å, but judging from the map quality and observable structural features, it appears that the orientational bias (Supplementary Figure S1B) and structural heterogeneity lead to an apparent resolution in the range of 8-9 Å and a wide range of local resolutions (Supplementary Figure S1C and Supplementary Table ST1). Nonetheless, the map quality allowed us to unambiguously place two RHD domains that were not observed in the previous CtUba4_{C202K}-CtUrm1 crystal structure and to determine their orientation (Figure 1D). Furthermore, we used rigid-body fitting followed by molecular dynamics flexible fitting to refine the obtained model (35) (Supplementary Figure S1A). Strikingly, predicted structural models of CtUba4, ScUba4 and HsMOCS3 (the human Uba4 homolog) by AlphaFold2 (36) position the RHD domain in a similar position and orientation, providing complementary support for our interpretation of the intermediate resolution cryo-EM maps (Supplementary Figure S2). Of note, we tested several approaches to further improve our reconstruction, but the relatively small size, structural heterogeneity and orientational bias (Supplementary Figure S1B) prevented us from reaching better quality maps. However, the obtained resolution and map quality allow us to observe that the RHD domain of CtUba4 is positioned in close proximity to the C-terminus of CtUrm1 (Figure 2A). In the AlphaFold models of CtUba4-Urm1, ScUba4-Urm1 and HsMOCS3-URM1 (Supplementary Figure S2), the catalytic cysteine of the RHD domain of Uba4 points towards the C-terminus of Urm1. In particular, the catalytic cysteine of the RHD domain in ScUba4 (Cys397) is positioned \sim 25 Å away from the C-terminus of Urm1. It is very likely that both, the RHD domain (with Cys397) as well as the C-terminus of Urm1, still undergo certain conformational changes during the actual thiocarboxylation reaction, and the observed relative positioning represents a pre-catalytically intermediate.

Functional validation of the interface between RHD domains and the Uba4-Urm1 complex

In the AlphaFold2 model of ScUba4-ScUrm1 complex, we inspected the interface between RHD domain and AD in Uba4, as well as RHD domain and Urm1 and identified a series of

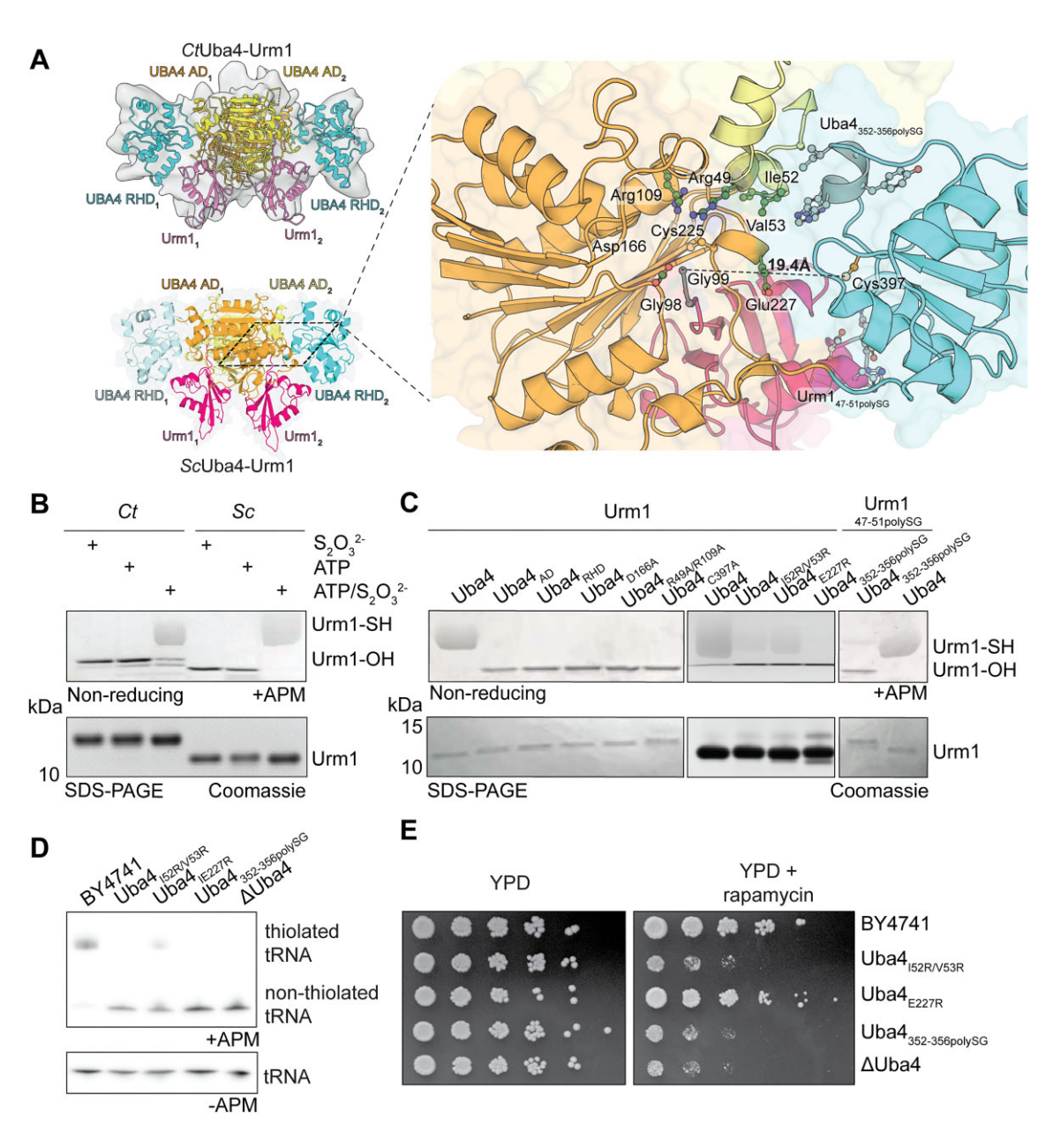


Figure 2. Residues at the interface between the AD-Urm1 complex and the RHD domain of Uba4 are essential for thiocarboxylation of Urm1 and tRNA thiolation. (**A**) Atomic model of *Ct*Uba4_{C202K}-*Ct*Urm1 fitted to the cryo-EM map (top) and the AlphaFold model of the *Sc*Uba4-*Sc*Urm1 complex (bottom). Close-up view on the *Sc*Uba4-*Sc*Urm1 model showing the position of conserved residues localized in the interface between RHD domain and Urm1. The distance between Gly99 and Cys397 is marked. (**B**) *In vitro* thiocarboxylation assay performed with purified *Ct*Uba4 and Urm1, or *Sc*Uba4 and Urm1 proteins. Urm1-SH can be produced in both cases, visible as a shifted band on the APM gel. (**C**) Thiocarboxylation assay with mutated variants of purified *Sc*Uba4 and *Sc*Urm1 proteins. Individual domains of Uba4 are not able to produce Urm1-SH (Uba4_{AD} and Uba4_{RHD}), and mutations in the adenylation site (Uba4_{D166A}, Uba4_{R49A/R109A}) or Uba4_{C397A} result in loss of thiocarboxylation activity. (**D**) Analysis of intracellular levels of thiolated tRNA_{Glu} in yeast strains carrying different variants of Uba4. Isolated tRNAs were separated by APM-supplemented (top) and regular urea-PAGE and visualed by northern blotting using a probe specific for tRNA_{Glu}. (**E**) Phenotypical analysis of Uba4 yeast mutants using tolerance to rapamycin. Rapamycin sensitivity is indicative of increased levels of hypomodified tRNAs. Yeast viability was assayed on YPD supplemented with 3 nM rapamycin at 30°C.

conserved residues that appeared to define the position of the RHD domain (Figure 2A). To study the role of these residues *in vitro* and *in vivo*, we used *S. cerevisiae* as a model system. Using APM-based SDS PAGE analyses, we confirmed similar ATP-dependent Urm1 thiocarboxylation activities for purified *Ct*Uba4 and *Sc*Uba4 *in vitro*. Of note, we used thiosulfate as a sulfur source for Uba4, which makes it possible to bypass Nfs1 and Tum1 ((37) and Figure 1A) to monitor thiocarboxylation of Urm1 *in vitro* (Figure 2B). The APM in the gel leads to an increased retardation of exposed thiol groups, which al-

lows to separate carboxylated from thiocarboxylated Urm1 (17,38).

Next, we purified several proteins mutated at residues likely belonging to the *Sc*Uba4-*Sc*Urm1 interface (Uba4 _{I52R/V53R}, Uba4_{E227R}, Uba4_{352-356polySG} and Urm1_{47-51polySG}) and tested their effects on Urm1 thiocarboxylation *in vitro*. We used the isolated AD and RHD domains as well as previously characterized mutations in the AD (Uba4_{D166A}, Uba4_{R49A/R109A}) and in the RHD domain (Uba4_{C397A}) (31) as negative controls. *Sc*Uba4_{I52R/V53R} and *Sc*Uba4_{352-356polySG} resulted in a strongly

decreased thiocarboxylation activity (Figure 2C), similar to the previously characterized loss-of-function mutations (31). In contrast, the activity of a ScUba4_{E227R} mutant was strongly affected, but still detectable. Of note, the mutation of a loop region in Urm1 (Urm1_{47-51polySG}) did not lead to any reduction of thiocarboxylation activity in vitro (Figure 2C). The same mutations led to similar effects in tRNA thiolation levels in vivo. ScUba4_{I51R/V52R} and ScUba4_{352-356polySG} almost completely lost thiolated tRNAGlu and ScUba4E227R showed a strong decrease (Figure 2D). All mutations also exhibited sensitivity to rapamycin, a hallmark of decreased tRNA modification levels (10), consistent with reduced tRNA thiolation (Figure 2E). In summary, our results show that residues found on both sides of the interface between AD, RHD domain and Urm1 are crucial for the Urm1 thiocarboxylation activity of Uba4 in vitro and in vivo. Although the possibility that these residues also play roles in different reaction steps remains, we suggest that they mediate the appropriate positioning of the RHD domain close to the C-terminus of Urm1 during the final thiocarboxylation step.

Canonical thiocarboxylation reaction only requires two conserved cysteines in AD and RHD domains

Our previous work on the interaction of Uba4 and Urm1 identified ATP as a co-factor for promoting complex formation between Uba4 and Urm1 (31). This observation mirrors the interaction between other eukaryotic E1 enzymes and their UBLs (21). In the reaction cycle of Uba4, the adenylated form of Urm1 is immediately subjected to a nucleophilic attack by the most proximal catalytic cysteine (Cys202 of CtUba4), resulting in the formation of a thioester intermediate, which is a common feature of essentially all eukaryotic E1-UBL systems (22). Therefore, the addition of DTT, which can resolve the thioester bond between Urm1 and Uba4 (37), almost completely dissociated Urm1 from the Uba4-Urm1 complex, suggesting that the thioester intermediate can be attacked by DTT resulting in the release of Urm1 from the complex (Figure 3A). The binding of Urm1 to a Uba4_{C202A} mutant is ATP-dependent, despite being incapable of forming the thioester intermediate with Urm1 (31). This suggests that the adenylation of Urm1 might be sufficient for complex stabilization. However, the addition of DTT, which affects thioester formation but not adenylation, resulted in complete complex dissociation (Figure 3A). These results suggest that in the absence of Cys202 a thioester bond can be formed between Urm1 and one or more cysteine residues in proximity of the adenylated C-terminus. A detailed structural analysis of the adenylation site showed the presence of several conserved cysteines, which are potential targets of alternative thioesterification reactions (Figure 3B). Therefore, we performed a systematic mutational analyses of all identified cysteines and combinations thereof and monitored formation of the Uba4-Urm1 thioester complex and thiocarboxylation of Urm1 in vitro. First, we confirmed that the formed thioester intermediate between CtUba4 and CtUrm1 indeed depends on the addition of ATP and that it can be resolved by hydroxylamine (Figure 3C and (37)). Of note, only a fraction of the purified components forms thioesters at a time and even high concentrations of ATP did not result in the equimolar thioester formation (Supplementary Figure S3A). Strikingly, thioester formation between Uba4 and Urm1 only occurred

when Cys202 was present, unambiguously confirming that this residue is the only physiological site for thioesterification (Figure 3C). Urm1-SH formation only occurred when both catalytic cysteines of *Ct*Uba4 (i.e. Cys202 and Cys397) were functional, underscoring their crucial role in the reaction cycle (Figure 3C).

Thioester intermediate protects the Urm1 from off-target conjugation

However, in the absence of alternative thioester attachment sites, the DTT-sensitive dissociation of Urm1 from Uba4_{C202A} in the pulldown assay remained elusive. Therefore, we further investigated the effect of DTT on complex formation between Urm1 and Uba4_{WT} or Uba4_{C202A} in solution, using SEC (Supplementary Figure S4A). The addition of DTT promoted the dissociation of Urm1 from the Uba4-Urm1 complex in both cases (Figure 4A), as well as a shift in the retention volume of Uba4 in the SEC profile (Supplementary Figure S4A). Strikingly, the liberated Urm1 molecules were shifted during electrophoresis, suggesting the modification of Urm1 during the release. We analyzed the samples in solution by mass spectrometry and identified the formation of a DTT adduct at the C-terminus of Urm1 (Figure 4B), reminiscent of the DTTadduct formation identified on TtuB (39). Of note, adenylated Urm1-AMP can be detected for both, Uba4_{WT} and Uba4_{C202A}, in the absence of DTT. Therefore, the Urm1-DTT adduct likely comes from the direct attack of Urm1-AMP by DTT (Figure 4B). The incubation with DTT and ATP leads to the formation of the Urm1-DTT adduct, but the use of the non-hydrolysable ATP analog AMPNPP in combination with DTT does not (Supplementary Figure S4B and D). Therefore, the formation of the adenylate intermediate is necessary for the formation of Urm1-DTT adducts.

DTT has been previously shown to rescue the in vitro thiocarboxylation activity of the otherwise inactive ScUba4C225A and ScUba4_{C397A} mutants (of note Cys202 and Cys397 in CtUba4 correspond to Cys225 and Cys397 in ScUba4) via an unknown reaction mechanism (22). We confirm here that the addition of DTT can indeed restore the formation of thiocarboxylated Urm1 of ScUba4C225A and ScUba4C397A in a concentration-dependent manner (Figure 4C). We were able to rescue the activity of ScUba4_{C225A} using approximately 10 μM DTT, corresponding to a 1:1 protein/DTT ratio, whereas ScUba4_{C397A} required a high excess of DTT (>1 mM). Therefore, we suggest that, for ScUba4C225A, Cys397 in the RHD domain can recognize and act on the Urm1-DTT thioester adduct, producing thiocarboxylated Urm1. The mechanism of DTT-driven rescue for Uba4_{C397A} is less clear, but likely requires the generation of polysulfides in the solution in vitro, which can lead to disulfide-exchange with the Urm1-DTT adduct, resulting in an artificial thiocarboxylation at high DTT concentrations. DTT is commonly used in the majority of Ubl reactions to ensure that cysteine residues are reduced (40), which also go through an initial adenylate intermediate. We detected the appearance of ubiquitin-DTT adducts during the reaction between UBE1 with ubiquitin in the presence of DTT (Supplementary Figure S4C). The formation of these adducts is also dependent on the adenylate intermediate, as they were undetectable after using AMPNPP (Supplementary Figure S4C and D). These results suggest that the use of DTT needs to be considered with particular care

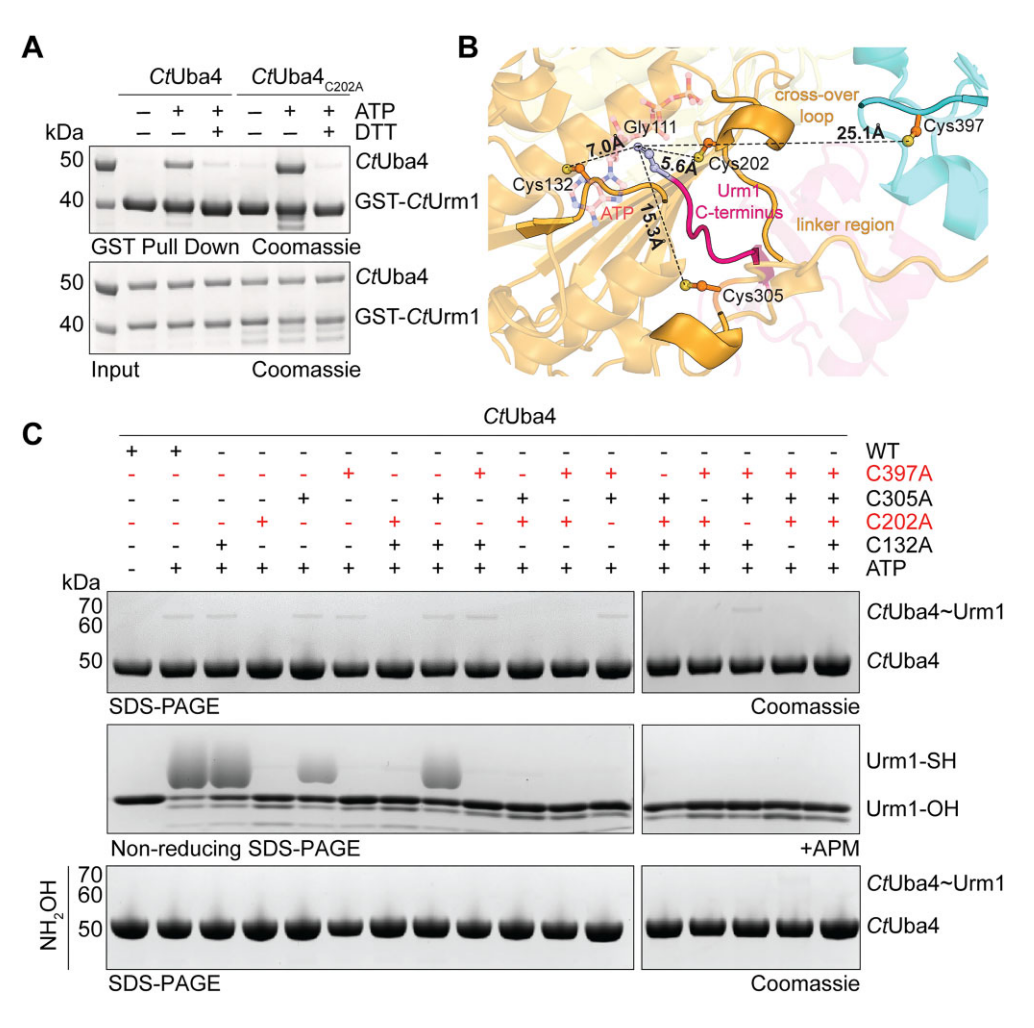


Figure 3. The two known catalytic cysteines in AD and RHD domains of CtUba4 are required for thiocarboxylation of Urm1 in vitro. (A) A GST-pulldown assay shows that the presence of ATP is needed for the interaction between CtUba4 and CtUrm1. Urm1 binding to Uba4_{C202A} is affected by DTT, suggesting the formation of alternative thioester intermediates. (B) Close-up view on the CtUba4-CtUrm1 model showing the position of the C-terminus of Urm1 and all cysteine residues in its proximity. The distances between individual cysteine residues and the C-terminus of Urm1 are marked. (C) Analyses of the capacity of individual CtUba4 variants to form, together with CtUrm1, a thioester intermediate and generate thiocarboxylated CtUrm1 and sensitivity of the analyzed complexes against hydroxylamine. All samples were analyzed for the formation of a thioester intermediate (top, SDS-PAGE), thiocarboxylated Urm1 (middle, Non-reducing SDS-PAGE + APM) and their sensitivity against hydroxylamine (bottom, +NH₂OH, SDS-PAGE). Variants carrying mutations in the catalytical residues are marked in red. The band corresponding to the thioester intermediate (CtUba4~CtUrm1), carboxylated Urm1 (Urm1-OH) and thiocarboxylated Urm1 (Urm1-SH) are marked.

when working with Ubl-AMP intermediates that show a similar potential to form DTT adducts. Furthermore, we analyzed the ability of Uba4 to use different sources of sulfur for the thiocarboxylation reaction, including thiosulfate, 3mercaptopyruvate (3-MP) and L-Cys. Both thiosulfate and 3-MP resulted in the canonical generation of Urm1-SH (Figure 4D). Addition of L-Cys resulted in a dramatic shift of Urm1 to the top of the APM-supplemented SDS-PAGE gels, suggesting the formation of a L-Cys adduct at the C-terminus of Urm1. Mass spectrometry analysis revealed that L-Cys forms an adduct on Urm1, mimicking the thioester formed at Cys202 (CtUba4) or Cys225 (ScUba4) (Supplementary Figure S3B). In summary, our results demonstrate that Urm1-AMP is capable of driving Urm1 to attach to various ligands (Figure 4E and Supplementary Figure S3B). Therefore, a highenergy bond, like the canonical thioester at the catalytic cysteine of the AD provides a much more stable intermediate to guarantee the proper generation of Urm1-SH, rather than Urm1-AMP.

Release of thiocarboxylated Urm1 does not require an exogenous reductant

Motivated by our understanding of the alternative (artificial) routes of Urm1-SH generation by Uba4, we were curious to know how Uba4 releases Urm1-SH at the end of the canonical reaction cycle. Acyl-disulfide is the last reaction intermediate formed during the thiocarboxylation cycle and has been identified for the ThiS-ThiF complex (41). After the persulfide on Cys397 in the RHD domain performs a nucleophilic attack on the Urm1-Uba4 thioester, a reducing agent is required to induce the cleavage of the produced acyl-disulfide. However, the mechanism that leads to the specific cleavage of this intermediate and release of Urm1-SH from Uba4 remains uncharacterized. Strikingly, we observed that Urm1-SH remained bound to Uba4, despite the presence of reducing agent which cleaves acyl-disulfides (Supplementary Figure S3C). To further characterize the release step of the reaction, we monitored the formation of thiocarboxylated Urm1 after mixing Uba4 and Urm1 at varying concentrations in the absence of

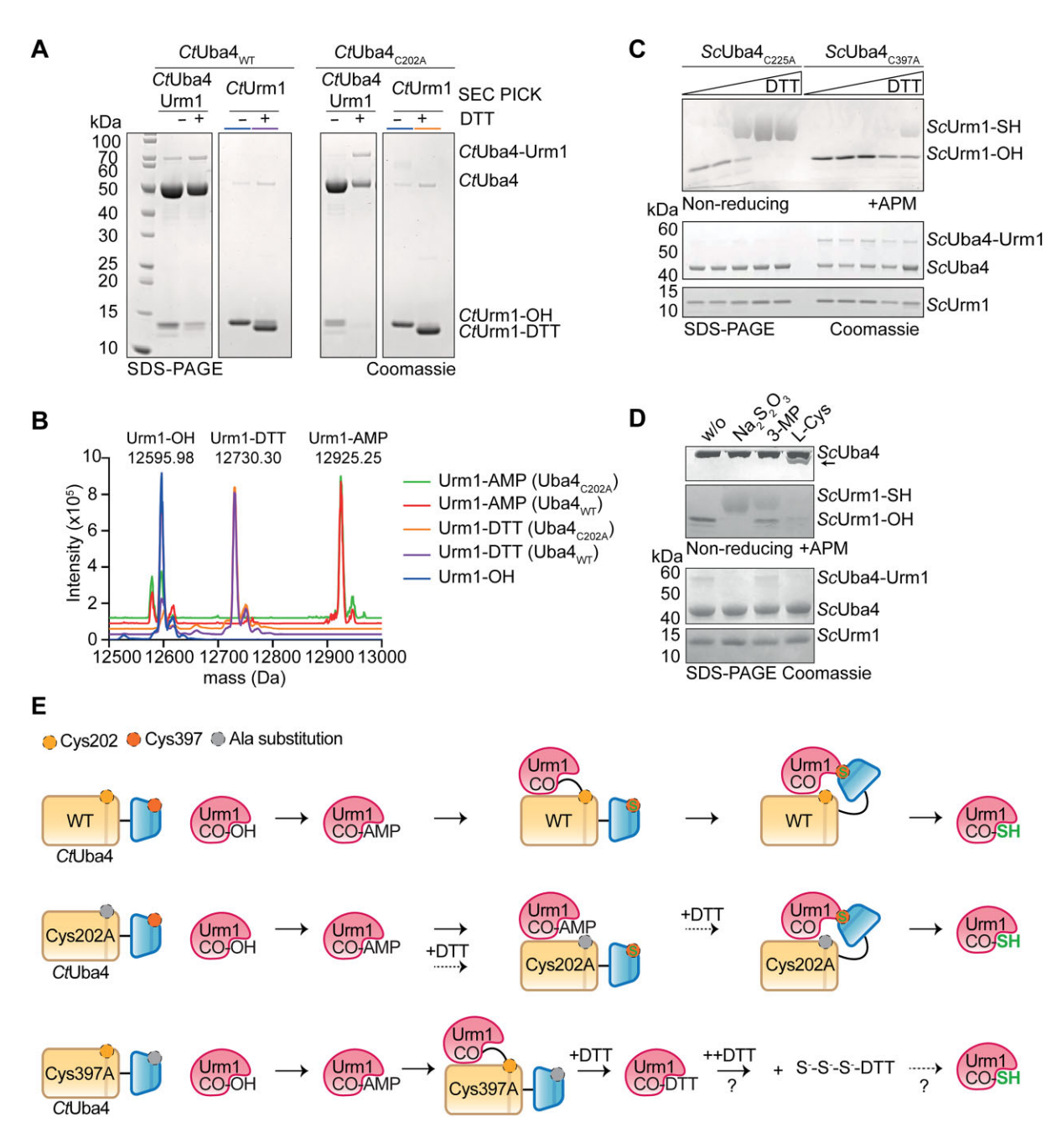


Figure 4. The adenylated C-terminus of Urm1 is prone to form DTT adducts. (A) SDS-PAGE analyses of the two peaks after SEC chromatography of Urm1 after incubation with CtUba4_{WT} or CtUba4_{C202A} in the presence of ATP, showing the peak of the Uba4-Urm1 complex and the free Urm1 peak in the presence and absence of DTT. Addition of DTT during the thioesterification reaction results in Urm1-DTT adduct formation and release of Urm1 from either CtUba4WT or CtUba4C202A. The presence of DTT changes the migration behavior of Urm1 on the SDS-PAGE gel, indicating the formation of an Urm1-DTT adduct. Samples analyzed by mass spectrometry in panel (B) are indicated by matching color. The corresponding SEC profile is shown in Supplementary Figure S4A. (B) Mass spectrometry analyses of the indicated samples from (A), showing the formation of Urm1-DTT adducts from Urm1-AMP precursor. Urm1-DTT adducts are also formed by Uba4_{C202A}, where thioesterification cannot take place. (C) Analyses of DTT-driven thiocarboxylation of Urm1 by ScUba4 mutants, by SDS-PAGE. In ScUba4_{C225A} (where Cys397 is present) the RHD domain can recognize Urm1-DTT adducts and thiocarboxylate them. In ScUb4_{C397A} higher concentrations of DTT are needed to generate Urm1-SH via an alternative RHD-independent route. (D) Analyses of alternative sulfur sources for thiocarboxylation by ScUba4 using SDS-PAGE. Thiosulfate and 3-MP can provide sulfur for the thiocarboxylation of Urm1 (ScUrm1-SH), whereas addition of Lcysteine results in the formation of an Urm1-L-Cys thioester on Uba4 (black arrow). (E) Schematic representation of the different reaction routes using the same depiction as in Figure 1A. In the canonical reaction by Uba4_{WT} (top), the adenylate is immediately converted into a thioester, which can be thiocarboxylated by the persulfidated cysteine in the RHD domain (Cys397). In the absence of Cys202, the thioester between CtUba4 and Urm1 cannot be formed, but DTT can perform a nucleic attack on the adenylate intermediate forming a Urm1-DTT adduct that can also be thiocarboxylated by the persulfidated RHD domain (middle). In the absence of Cys397, higher concentrations of DTT can also lead to the thiocarboxylation of Urm1 via an alternative, RHD-independent and currently unknown reaction (bottom).

reducing agents (Figure 5A). At a 1:1 molar ratio between a one Urm1 molecule and one Uba4 dimer, Urm1 is fully converted to Urm1-SH even in the absence of reducing agents. If additional Urm1 is added to the reaction, it is no longer converted into Urm1-SH and any additional Urm1 remains in its carboxylated form. Therefore, exogenous reductants are required for reaction turnover *in vitro* but are dispensable for the generation of Urm1-SH. Our results also show that the cleavage of the acyl-disulfide by reducing agents is not sufficient to trigger Urm1-SH release from the complex.

We hypothesized that the release of Urm1-SH might be driven by the arrival of the next Urm1 molecule. While not strictly required (42), adenylation of a second Ubiguitin molecule has been found to promote the transthioesterification of an already E1-bound ubiquitin molecule (21,43). Considering that Uba4-Urm1 complex is comprised of potentially two active adenylation sites, we were interested to find out if binding of another Urm1 molecule impacts the reactivity of the processed Urm1. To assess this possibility for Urm1, we first performed the thiocarboxylation of Urm1 in the absence of reducing agent and isolated free and Uba4bound Urm1 by SEC (Figure 5B). As expected, Urm1-SH was efficiently formed and remained tightly bound to Uba4. Next, we removed ATP and thiosulfate to avoid the formation of new Urm1-SH and added an excess of fresh Urm1. The subsequent analyses showed that most (if not all) of Urm1-SH gets released from Uba4 (Figure 5B) Since Urm1-SH generation was only allowed to occur in the first incubation stage, the release of Urm1-SH from Uba4 was driven by the binding of unprocessed Urm1 (Figure 5C).

Integration of the Uba4/Urm1 reaction cycle in the eukaryotic thiolation cascade

Upon release from Uba4, Urm1-SH is subsequently involved in two downstream pathways: (i) the canonical tRNA modification thiolation cascade (10) or (ii) the UBL-like conjugation to target proteins, also known as urmylation (15,17). The latter requires no additional factors other than an oxidized cysteine residues in the respective target proteins. The complex comprises Ncs2 and Ncs6 is required for the s²U₃₄ modification in vivo. However, a detailed analysis of the downstream sulfur transfer to tRNAs in vitro has been hindered by the inability to purify the eukaryotic Ncs2/Ncs6 complex. We have recently established the purification of Ncs2 and Ncs6 from the fungus C. thermophilum (44). First, we confirmed by isothermal titration calorimetry (ITC) that the individually purified Ncs2 and Ncs6 proteins form a stable complex with high affinity ($k_d = \sim 150$ nM; Figure 6A and Supplementary Figure S4E). Next, we used GST-pull down assays to test the interaction of CtUrm1 with CtNcs2, CtNcs6 and the reconstituted CtNcs2/CtNcs6 complex. Urm1 specifically interacts only with Ncs6, but not with Ncs2 or the reconstituted Ncs2/Ncs6 complex (Figure 6B). In EMSA assays, CtNcs2, CtNcs6 and the reconstituted CtNcs2/CtNcs6 complex bind in vitro transcribed tRNAGIn with affinities comparable to other tRNA-binding proteins (45-48), showing that CtNcs2 and the CtNcs2/CtNcs6 in principle bind the expected substrate (Supplementary Figure S4F). To understand the molecular mechanisms that prevent Urm1 from binding to Ncs2 and the Ncs2/Ncs6 complex, as well as the specific interface formed between Urm1 and Ncs6, will require additional structural work in the future.

Upstream of Uba4, Tum1 (or 3-mercaptopyruvate sulfurtransferase [MPST] in humans) is required for persulfide formation at the catalytic cysteine residue in the RHD domain, and it was recently confirmed that MPST can indeed transfer persulfide to Uba4 in vitro (49). However, it was also shown that the loss of Tum1 in yeast strains only leads to a partial decrease in the s^2U_{34} tRNA modification levels (50,51), questioning the essential requirement for relaying sulfur to Uba4 via Tum1. Tum1 itself harbors a RHD domain fold, which is highly similar to the RHD domain of Uba4 and is critical for its ability to accept sulfur from 3-mercaptopyruvate (3MP) and deliver persulfides to target proteins and other molecules (49). The intermediate tRNA modification phenotype of the Tum1 knockout in yeast (52) and the apparent redundancy between Tum1 and the RHD domain of Uba4 urged us to investigate the role of Tum1 for the thiocarboxylation activity of Uba4 in vitro. We tested the ability of Tum1 to rescue inactive mutants of Uba4 (Figure 6C). Indeed, Tum1 was capable of partially rescuing the production of Urm1-SH when both critical cysteines (C225 and C397) are mutated, whereas an active site mutant of Tum1 (Tum1_{C259S}) failed to promote thiocarboxylation of Urm1. These results indicate that Tum1 can not only act as a backup RHD module in the thiocarboxylation reaction, but even directly attack the Urm1-AMP intermediate, which would be reminiscent of prokaryotic SCPs where no thioester intermediate is present (53). We speculate that in the case of deleting Tum1 in yeast, the RHD domain of Uba4 still gets charged with sulfur by other yet unknown factors, which permits the production of Urm1-SH and thiolate tRNAs (52). However, the canonical route via Tum1 is likely more efficient, which causes the decreased level of tRNA modification in the deletion strain. In summary, our result show that the reaction cycle of Uba4/Urm1 is tightly connected to the upstream and downstream factors and additional work will be required to reveal how sulfur is directed into the reaction cycle under varying environmental conditions (e.g. with limited intracellular sulfur levels and oxidative stress).

Discussion

Our study sought to describe previously unknown mechanistic details of the thiocarboxylation reaction of Urm1 by Uba4 and its release at the end of the reaction cycle. As Urm1 and its E1-activating enzyme Uba4 represent an evolutionary branch point between prokaryotic SCPs and eukaryotic UBLs, our results allow a detailed molecular comparison between both related protein families. Furthermore, our work paves the way to understanding the evolutionary processes that ultimately led to the development of the highly complex UBL-conjugation systems. During the preparation of this manuscript, it was shown that both, Urm1 and Uba4, are involved in the formation of stress-dependent condensate formation in yeast (54). As Uba4 and Urm1 appear to enter these condensates bound to each other, it remains to be shown whether the molecular mechanisms presented here are critical for the formation and resolution of these phase-separated condensates in different organisms.

We performed the cryo-EM reconstruction of the Uba4/Urm1 complex at a resolution up to 5.9 Å, which reveals the proximal positioning of the RHD domains of Uba4 during the final reaction step. In addition, our cryo-EM dataset contains particles resembling both previously characterized intermediates of Uba4, namely apo CtUba4_{C202K} and

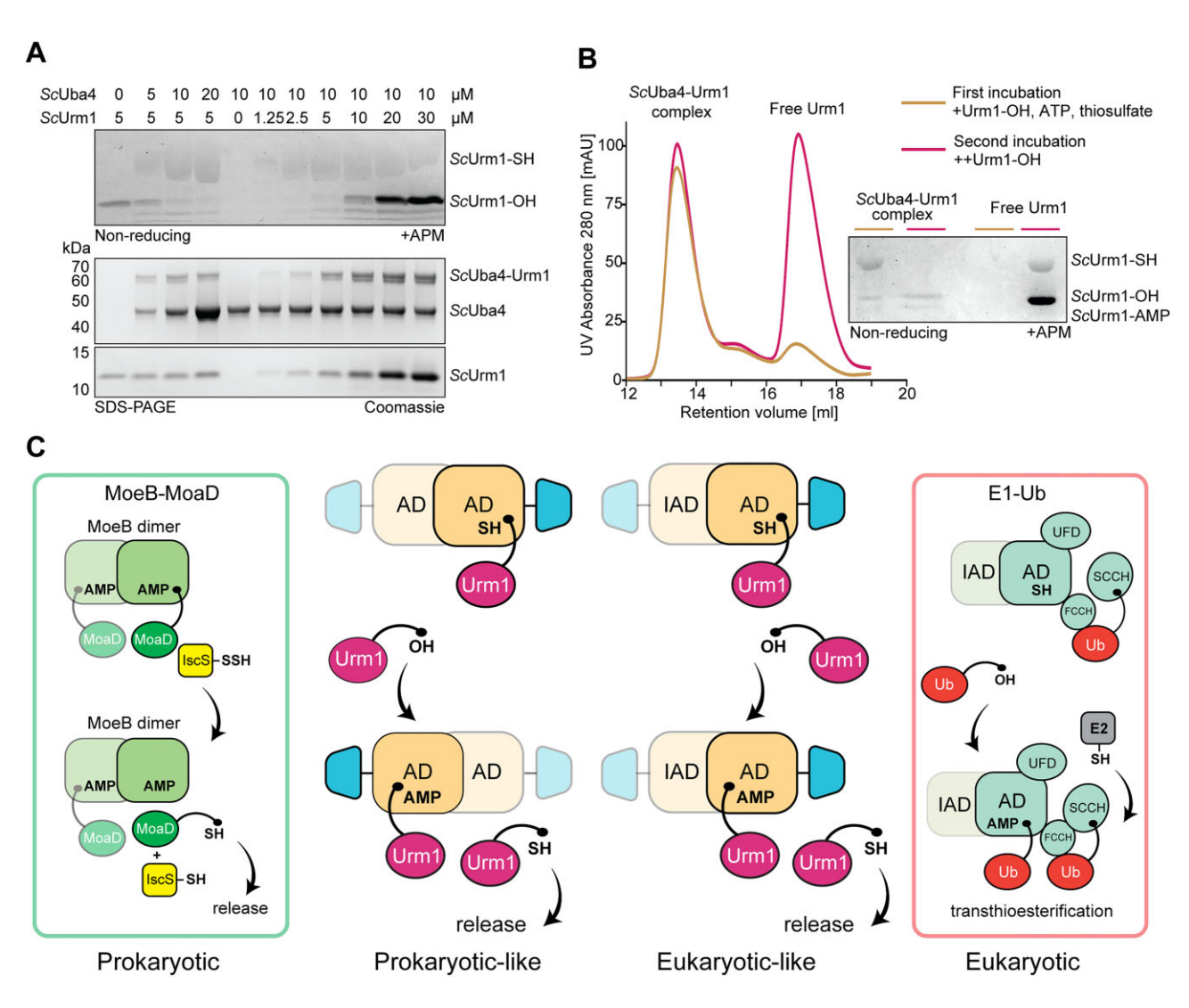


Figure 5. The release of Urm1-SH from Uba4 is driven by incoming Urm1-OH. (A) Monitoring of *in vitro* formation of thiocarboxylated *Sc*Urm1 in the absence of reducing agents by APM-based SDS-PAGE. Urm1-SH is formed at molar ratios between *Sc*Uba4 and Urm1, corresponding to a Uba4 dimer reacting with a single Urm1. Excess of Urm1 does not lead to the additional formation of Urm1-SH but accumulation of non-reacted Urm1-OH. (B) Analyses of release of Urm1 after its thiocarboxylation using SEC. During the first incubation, Uba4 thiocarboxylates Urm1 in the absence of a reducing agent, but the complex cannot dissociate. After removal of ATP and sulfur an excess of Urm1-OH was added, which can displace Urm1-SH from *Sc*Uba4. (C) Schematic representation of two possible scenarios for Urm1 release and their comparison to established release mechanisms from prokaryotic SCP and eukaryotic E1-UBL systems. AD, active adenylation domain; FCCH, first catalytic cysteine half-domain; IAD, inactive adenylation domain; SCCH, second catalytic cysteine half-domain; UFD, ubiquitin-fold domain.

the CtUba4_{C202K}-CtUrm1 complex, where the RHD domains are flexible. Of note, no degradation or proteolytic cleavage of the RHD domain was detected during crystallization or cryo-EM sample preparation, indicating a dynamic equilibrium between the different positions of the RHD domains. Furthermore, unconjugated CtUba4_{C202K} is still observable on SDS-PAGE gels, even after SEC-based repurification of the conjugation products, explaining the observed heterogeneity in our cryo-EM analyses (Figure 1B). Our structural results suggest that Urm1 and its C-terminus can remain bound to Uba4 in an almost identical position during adenylation, thioester formation and thiocarboxylation. As predicted, the previously observed dimer of the RHD domain is indeed dissociated upon Urm1 binding and the two RHD domains undergo a large conformational change that brings their persulfided cysteine residues in proximity of Urm1's C-termini. Currently, it is unclear at which exact stage Tum1 transfers

the activated sulfur moiety to the active site cysteine of the RHD domain, because this residue is not accessible in the dimer of the RHD domains (31). However, it is likely that formation of the persulfide in the RHD domain happens after dimer dissociation. Finally, we show that Tum1 appears to be able to substitute for the RHD domain of Uba4 and deliver sulfur directly to the C-terminus of Uba4-bound Urm1.

Remarkably, Urm1-SH is autonomously produced by a single Uba4 dimer without external reductants. In the absence of reductants, only one Urm1-SH molecule is generated, while additional Urm1 molecules are trapped at the Urm1-AMP or thioester stage due to the unavailability of catalytic Cys397. The homodimeric Uba4-Urm1 complex exhibits two active ADs, potentially allowing for the simultaneous binding of a second Urm1 molecule. Therefore, two distinct mechanisms can be envisioned: a prokaryotic-like mechanism that would take advantage of both active ADs, and a eukaryotic-

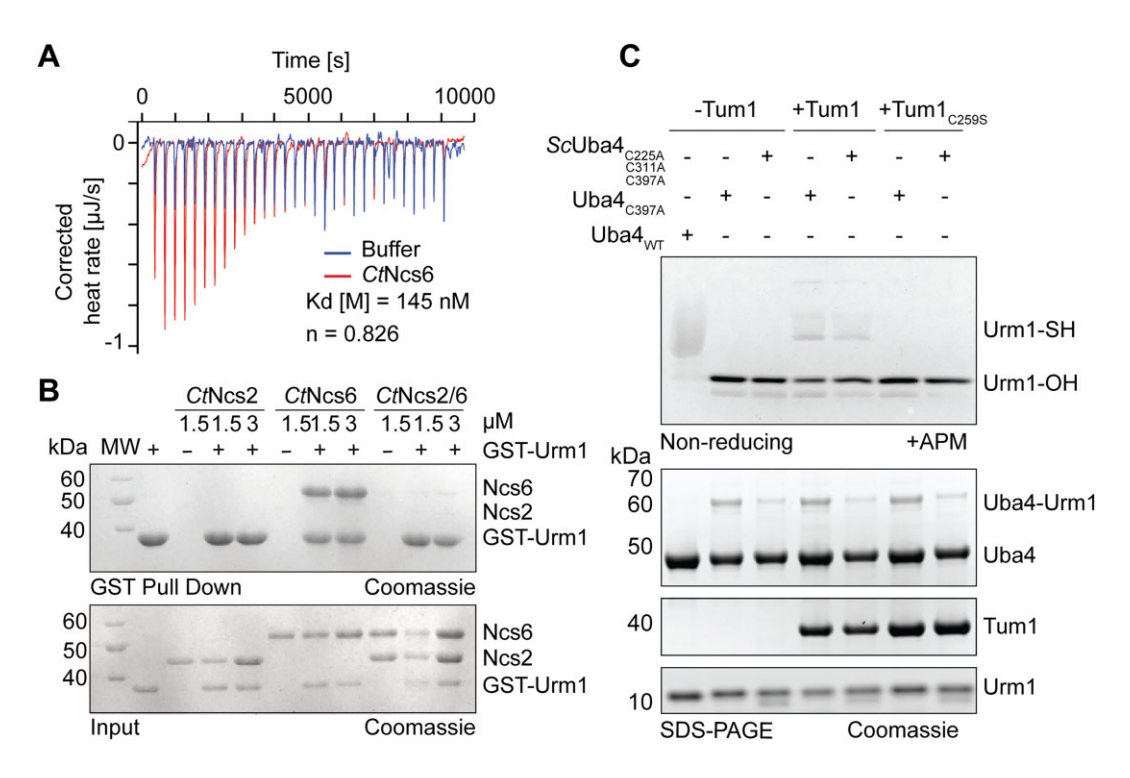


Figure 6. Urm1 interacts with Ncs6 but not with Ncs2 or the Ncs2/Ncs6 complex, and Tum1 can partially complement for the RHD domain of Uba4. (**A**) ITC analyses of the interaction between purified *Ct*Ncs2 and *Ct*Ncs6. ITC peak profiles of the titrated buffer and *Ct*Ncs6 are shown together with the derived parameters of the binding. (**B**) GST-pulldown interaction assay showing that purified GST-Urm1 is binding to purified *Ct*Ncs6, but not to *Ct*Ncs2 or *Ct*Ncs2/Ncs6. Samples and controls were analyzed by SDS-PAGE. (**C**) Purified yeast Tum1 is able to partially restore the thiocarboxylation activity of *Sc*Uba4 mutants, lacking the catalytic cysteine (Cys397) in the RHD domain. The Tum1_{C259S} mutant lacking the catalytic cysteine is not able to rescue the activity under the same conditions. Samples and loading controls were analyzed by SDS-PAGE and APM-based SDS-PAGE.

like mechanism where the asymmetry of the AD-RHD domain dimeric assembly would favor only one active AD site (Figure 5C). The first prokaryotic-like scenario, supported by structures of MoeB/MoaD (55), ThiS-ThiF (56), and the Uba4/Urm1 complex, involves the alternating binding of UBL molecules to both AD in the E1 dimer, resembling a pingpong mechanism (Figure 5C). In the second eukaryotic-like scenario, binding of the second Urm1 molecule prompts linker displacement, rearranging the first RHD domain. This model suggests a role for the first RHD domain akin to the first catalytic cysteine half-domain (FCCH) and second catalytic cysteine half-domain (SCCH) domains in Uba1, allowing adenylation of the second Urm1. However, the stark contrast between Uba4 and Uba1 is the proximity of the catalytic cysteine in the AD of Uba4 to the P-loop motif. Unlike Uba4, Uba1 promotes the displacement of the first Ubiquitin by placing the thioesterification site away from the AD. In both scenarios, the spontaneous cleavage of the acyl-disulfide, the final reaction intermediate, requires a second cysteine of Uba4 for nucleophilic attack, resulting in the production of Urm1-SH, and the formation of an intramolecular disulfide bond involving Cys397 and the additional cysteine driving cleavage and release (Figure 7). It remains to be shown, whether the release mechanism of Urm1 from Uba4 is closer related to prokaryotic SCP systems or eukaryotic UBL systems.

The capacity of UBLs to conjugate with target proteins is accompanied by the inherent risk of self-conjugation with their respective E1-enzymes during activation. For instance, adenylation of SAMP is sufficient to trigger self-conjugation in the UbaA/SAMP system, regardless of the presence of the active cysteine of UbaA (28). Addition of Urm1-SH to Uba4 that

has lost the possibility to form a thioester, leads to increased rates of self-urmylation (31). These observations highlight the volatility of the adenylated UBL intermediate and underline the advantage of converting the adenylate into a thioester linkage. In addition to the potential risk of self-conjugation, we observed that Urm1-AMP is also highly prone to form other C-terminal adducts, which adds yet another important reason to protect the C-terminus via a less reactive thioester until the RHD domain can thiocarboxylate it. This selective advantage that is absent in prokaryotic SCPs and for the first time observed in Urm1, might have promoted the use of thioester intermediates also in E2 conjugating enzymes and in certain families of E3 ligases.

Ncs6 harbors three conserved cysteine residues and is thought to orchestrate an iron sulfur cluster crucial for sulfur transfer from the C-terminus of Urm1 to tRNA as shown for the orthologous enzymes from human (57) and the archaeum *Methanoccus maripaludis* (58). The enigma of Ncs2, devoid of these cysteine residues, persists. Despite the absence of observed iron sulfur clusters in our purified Ncs6 preparations, the discerned specificity of Urm1-binding to the catalytically active subunit alludes to a specific interface formation between Urm1 and Ncs6 extending beyond the region around the iron sulfur cluster. The complexity of cellular thiolation cascades arises from sulfur's versatile behavior, influencing redox potential and reactivity in local environments.

In summary, our work consolidates the fundamental interplay between Urm1 and Uba4, which conduct the generation of a unique UBL that can relay sulfur to both proteins as well as tRNAs. Foremost, our work substantiates that the Uba4/Urm1 pair shares features from the prokaryotic SCP

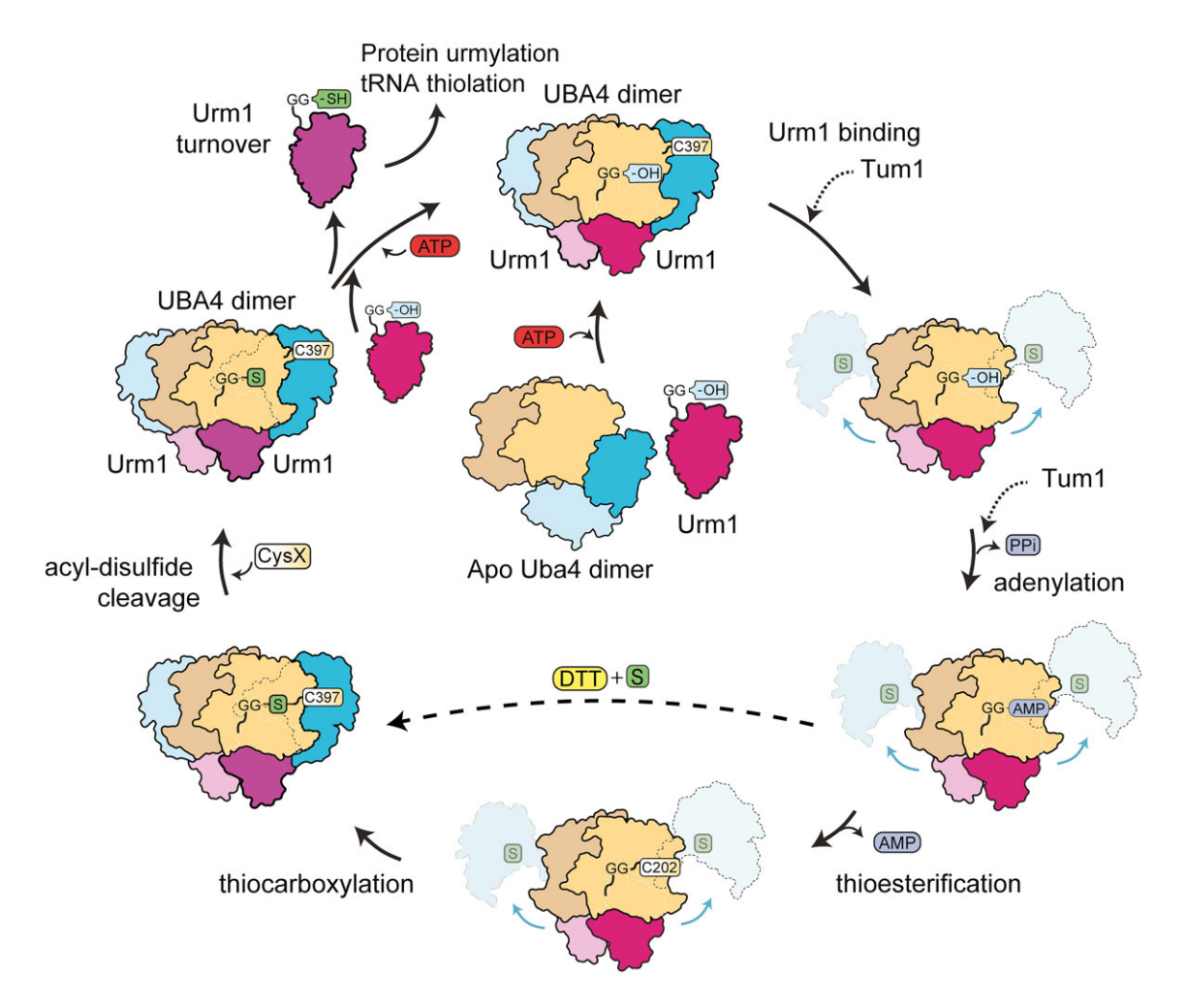


Figure 7. Schematic overview of the Urm1 thiocarboxylation reaction by Uba4. Upon Urm1 binding to the AD of Uba4, the dimer of RHD domains dissociates from the AD, and the individual domains are moving apart from each other. Urm1 is adenylated and subsequently forms a thioester intermediate with the catalytic cysteine in the AD of Uba4 (Cys202 in CtUba4). Tum1 can donate sulfur to the catalytic cysteine of the RHD domain or act as a secondary RHD domain in the thiocarboxylation reaction. Persulfidated Cys397 localized in the RHD domain, attacks the Urm1 carbonyl group, forming an acyl-disulfide, that undergoes spontaneous cleavage, as a result of a nucleophilic attack of a yet unidentified Uba4 cysteine group (CysX). Thiocarboxylated Urm1 is released upon binding of a fresh Urm1 molecule and Uba4 is able to restart the reaction cycle. Urm1-SH is used for tRNA thiolation, protein urmylation and cysteine persulfidation. DTT together with a sulfur donor can facilitate Urm1-SH formation, bypassing the steps of thioester formation and RHD-dependent thiocarboxylation.

world and the eukaryotic UBL world—defining it as unique system that fulfills crucial cellular functions and at the same time allowed the evolution of complex UBL systems.

Data availability

The reported cryo-EM map has been deposited with the EMDB under the accession number EMD-19967. The mass spectrometry data were deposited to the MassIVE repository with the dataset identifier MSV000094152. All other data generated in this study are available from corresponding authors on reasonable request.

Supplementary data

Supplementary Data are available at NAR Online.

Acknowledgements

We would like to thank Alicia Cordova Perez and Yogesh Kulathu (MRC PPU, University of Dundee, UK) for provid-

ing purified ubiquitin and UBE1. We would like to thank the whole Solaris team for their constant support during cryo-EM grid screening and sample optimization. We would also like to thank Brandán Pedre for his valuable insights into molecular mechanisms of sulfur transferases. In addition, we are grateful to all members of the Glatt lab for insightful discussion during the preparation of this manuscript. The work is supported under the Polish Ministry and Higher Education project: 'Support for research and development with the use of research infrastructure of the National Synchrotron Radiation Centre SOLARIS' under contract nr 1/SOL/2021/2.

Funding

European Research Council (ERC) [101001394 to S.G.]; Horizon Europe 2020 [101090314 to D.K.]; Fundacja na rzecz Nauki Polskiej [FirstTEAM/2016-1/2 to S.G.]; Schweizerischer Nationalfonds zur Förderung der Wissenschaftlichen Forschung [184947 to S.A.L.]. Funding for open access charge: Priority Research Area BioS under the

program 'Initiative of Excellence - Research University' at the Jagiellonian University in Krakow.

Conflict of interest statement

None declared.

References

- 1. Ranjan, N. and Rodnina, M.V. (2016) tRNA wobble modifications and protein homeostasis. *Translation (Austin)*, 4, e1143076.
- 2. Ranjan,N. and Rodnina,M.V. (2017) Thio-modification of tRNA at the wobble position as regulator of the kinetics of decoding and translocation on the ribosome. *J. Am. Chem. Soc.*, **139**, 5857–5864.
- Nedialkova, D.D. and Leidel, S.A. (2015) Optimization of codon translation rates via tRNA modifications maintains proteome integrity. *Cell*, 161, 1606–1618.
- Zinshteyn,B. and Gilbert,W.V. (2013) Loss of a conserved tRNA anticodon modification perturbs cellular signaling. *PLoS Genet.*, 9, e1003675.
- Laxman,S., Sutter,B.M., Wu,X., Kumar,S., Guo,X., Trudgian,D.C., Mirzaei,H. and Tu,B.P. (2013) Sulfur amino acids regulate translational capacity and metabolic homeostasis through modulation of tRNA thiolation. *Cell*, 154, 416–429.
- Alings,F., Sarin,L.P., Fufezan,C., Drexler,H.C. and Leidel,S.A. (2015) An evolutionary approach uncovers a diverse response of tRNA 2-thiolation to elevated temperatures in yeast. RNA, 21, 202–212.
- Damon, J.R., Pincus, D. and Ploegh, H.L. (2015) tRNA thiolation links translation to stress responses in *Saccharomyces cerevisiae*. *Mol. Biol. Cell*, 26, 270–282.
- 8. Bimai,O., Arragain,S. and Golinelli-Pimpaneau,B. (2020) Structure-based mechanistic insights into catalysis by tRNA thiolation enzymes. *Curr. Opin. Struct. Biol.*, 65, 69–78.
- Cavuzic, M. and Liu, Y. (2017) Biosynthesis of sulfur-containing tRNA modifications: a comparison of bacterial, archaeal, and eukaryotic pathways. *Biomolecules*, 7, 27.
- Leidel, S., Pedrioli, P.G.A., Bucher, T., Brost, R., Costanzo, M., Schmidt, A., Aebersold, R., Boone, C., Hofmann, K. and Peter, M. (2009) Ubiquitin-related modifier Urm1 acts as a sulphur carrier in thiolation of eukaryotic transfer RNA. *Nature*, 458, 228–232.
- Huang,B.O., Lu,J. and Bystro,A.S. (2008) A genome-wide screen identifies genes required for formation of the wobble nucleoside in Saccharomyces cerevisiae. RNA, 14, 2183–2194.
- Noma,A., Sakaguchi,Y. and Suzuki,T. (2009) Mechanistic characterization of the sulfur-relay system for eukaryotic 2-thiouridine biogenesis at tRNA wobble positions. *Nucleic Acids Res.*, 37, 1335–1352.
- Furukawa, K., Mizushima, N., Noda, T. and Ohsumi, Y. (2000) A
 protein conjugation system in yeast with homology to biosynthetic
 enzyme reaction of prokaryotes. *J. Biol. Chem.*, 275, 7462–7465.
- 14. Van Der Veen, A.G., Schorpp, K., Schlieker, C., Buti, L., Damon, J.R., Spooner, E., Ploegh, H.L. and Jentsch, S. (2011) Role of the ubiquitin-like protein Urm1 as a noncanonical lysine-directed protein modifier. *Proc. Natl Acad. Sci. U.S.A.*, 108, 1763–1770.
- Brachmann, C., Kaduhr, L., Jüdes, A., Ravichandran, K.E., West, J.D., Glatt, S. and Schaffrath, R. (2020) Redox requirements for ubiquitin-like urmylation of Ahp1, a 2-cys peroxiredoxin from yeast. Redox. Biol., 30, 101438.
- 16. Goehring, A.S., Rivers, D.M. and Sprague, G.F. (2003) Attachment of the ubiquitin-related protein Urm1p to the antioxidant protein Ahp1p. *Euk. Cell*, 2, 930–936.
- 17. Ravichandran,K.E., Kaduhr,L., Skupien-Rabian,B., Shvetsova,E., Sokołowski,M., Krutyhołowa,R., Kwasna,D., Brachmann,C., Lin,S., Guzman Perez,S., *et al.* (2022) E2 /E3 -independent ubiquitin-like protein conjugation by Urm1 is directly coupled to cysteine persulfidation. *EMBO J.*, 41, 1–23.

- 18. Kaduhr, L., Brachmann, C., Ravichandran, K.E., West, J.D., Glatt, S. and Schaffrath, R. (2021) Urm1, not quite a ubiquitin-like modifier? *Microb. Cell*, 8, 256–261.
- Xu,J., Zhang,J., Wang,L., Zhou,J., Huang,H., Wu,J., Zhong,Y. and Shi,Y. (2006) Solution structure of Urm1 and its implications for the origin of protein modifiers. *Proc. Natl Acad. Sci. U.S.A.*, 103, 11625–11630.
- Termathe, M. and Leidel, S.A. (2021) Urm1: a non-canonical ubl. Biomolecules, 11, 139.
- Lee, I. and Schindelin, H. (2008) Structural insights into E1-catalyzed ubiquitin activation and transfer to conjugating enzymes. Cell, 134, 268–278.
- 22. Termathe,M. and Leidel,S.A. (2018) The Uba4 domain interplay is mediated via a thioester that is critical for tRNA thiolation through Urm1 thiocarboxylation. *Nucleic Acids Res.*, 46, 5171–5181.
- 23. Marelja, Z., Stöcklein, W., Nimtz, M. and Leimkühler, S. (2008) A novel role for human Nfs1 in the cytoplasm: nfs1 acts as a sulfur donor for MOCS3, a protein involved in molybdenum cofactor biosynthesis. *J. Biol. Chem.*, 283, 25178–25185.
- 24. Chowdhury, M.M., Dosche, C., Löhmannsröben, H.-G. and Leimkühler, S. (2012) Dual role of the molybdenum cofactor biosynthesis protein MOCS3 in tRNA thiolation and molybdenum cofactor biosynthesis in humans. J. Biol. Chem., 287, 17297–17307.
- 25. Matthies, A., Nimtz, M. and Leimkühler, S. (2005) Molybdenum cofactor biosynthesis in humans: identification of a persulfide group in the rhodanese-like domain of MOCS3 by mass spectrometry. *Biochemistry*, 44, 7912–7920.
- Zhang, W., Urban, A., Mihara, H., Leimkühler, S., Kurihara, T. and Esaki, N. (2010) IscS functions as a primary sulfur-donating enzyme by interacting specifically with MoeB and MoaD in the biosynthesis of molybdopterin in *Escherichia coli*. J. Biol. Chem., 285, 2302–2308.
- 27. Dahl, J.-U., Radon, C., Bühning, M., Nimtz, M., Leichert, L.I., Denis, Y., Jourlin-Castelli, C., Iobbi-Nivol, C., Méjean, V. and Leimkühler, S. (2013) The sulfur carrier protein TusA has a pleiotropic role in *Escherichia coli* that also affects molybdenum cofactor biosynthesis. *J. Biol. Chem.*, 288, 5426–5442.
- 28. Hepowit, N.L., Vera, I.M.S., Cao, S., Fu, X., Wu, Y., Uthandi, S., Chavarria, N.E., Englert, M., Su, D., Söll, D., *et al.* (2016) Mechanistic insight into protein modification and sulfur mobilization activities of noncanonical E1 and associated ubiquitin-like proteins of Archaea. *FEBS J.*, 283, 3567–3586.
- Hepowit, N.L. and Maupin-Furlow, J.A. (2019) Rhodanese-like domain protein UbaC and its role in ubiquitin-like protein modification and sulfur mobilization in archaea. *J. Bacteriol.*, 201, e00254-19.
- Miranda, H.V., Nembhard, N., Su, D., Hepowit, N., Krause, D.J., Pritz, J.R., Phillips, C., Söll, D. and Maupin-Furlow, J.A. (2011) E1and ubiquitin-like proteins provide a direct link between protein conjugation and sulfur transfer in archaea. *Proc. Natl Acad. Sci.* U.S.A., 108, 4417–4422.
- 31. Pabis, M., Termathe, M., Ravichandran, K.E., Kienast, S.D., Krutyhołowa, R., Sokołowski, M., Jankowska, U., Grudnik, P., Leidel, S.A. and Glatt, S. (2020) Molecular basis for the bifunctional Uba4–Urm1 sulfur-relay system in tRNA thiolation and ubiquitin-like conjugation. EMBO J., 39, e105087.
- Tegunov,D. and Cramer,P. (2019) Real-time cryo-electron microscopy data preprocessing with Warp. *Nat. Methods*, 16, 1146–1152.
- 33. Yariv,B., Yariv,E., Kessel,A., Masrati,G., Chorin,A.B., Martz,E., Mayrose,I., Pupko,T. and Ben-Tal,N. (2023) Using evolutionary data to make sense of macromolecules with a 'face-lifted' ConSurf. *Protein Sci.*, 32, e4582.
- 34. Chramiec-Głąbik, A., Rawski, M., Glatt, S. and Lin, T.-Y. (2023) Electrophoretic mobility shift assay (EMSA) and microscale thermophoresis (MST) methods to measure interactions between tRNAs and their modifying enzymes. *Methods Mol. Biol.*, 2666, 29–53.

- 35. Kidmose,R.T., Juhl,J., Nissen,P., Boesen,T., Karlsen,J.L. and Pedersen,B.P. (2019) Namdinator automatic molecular dynamics flexible fitting of structural models into cryo-EM and crystallography experimental maps. *IUCrJ*, 6, 526–531.
- 36. Jumper, J., Evans, R., Pritzel, A., Green, T., Figurnov, M., Ronneberger, O., Tunyasuvunakool, K., Bates, R., Žídek, A., Potapenko, A., et al. (2021) Highly accurate protein structure prediction with AlphaFold. Nature, 596, 583–589.
- Termathe, M. and Leidel, S.A. (2018) The Uba4 domain interplay is mediated via a thioester that is critical for tRNA thiolation through Urm1 thiocarboxylation. *Nucleic Acids Res.*, 46, 5171–5181.
- 38. Lemau de Talancé, V., Bauer, F., Hermand, D. and Vincent, S.P. (2011) A simple synthesis of APM ([p-(N-acrylamino)-phenyl]mercuric chloride), a useful tool for the analysis of thiolated biomolecules. *Bioorg. Med. Chem. Lett.*, 21, 7265–7267.
- Shigi,N., Sakaguchi,Y., Asai,S.-I., Suzuki,T. and Watanabe,K. (2008) Common thiolation mechanism in the biosynthesis of tRNA thiouridine and sulphur-containing cofactors. EMBO J., 27, 3267–3278.
- Pickart, C.M. and Raasi, S. (2005) Controlled synthesis of polyubiquitin chains. *Methods Enzymol.*, 399, 21–36.
- Lehmann, C., Begley, T.P. and Ealick, S.E. (2006) Structure of the Escherichia coli This-ThiF complex, a key component of the sulfur transfer system in thiamin biosynthesis. *Biochemistry*, 45, 11–19.
- Pickart, C.M., Kasperek, E.M., Beal, R. and Kim, A. (1994) Substrate properties of site-specific mutant ubiquitin protein (G76A) reveal unexpected mechanistic features of ubiquitin-activating enzyme (E1). J. Biol. Chem., 269, 7115–7123.
- 43. Schäfer, A., Kuhn, M. and Schindelin, H. (2014) Structure of the ubiquitin-activating enzyme loaded with two ubiquitin molecules. *Acta. Crystallogr. D Biol. Crystallogr.*, 70, 1311–1320.
- 44. Alings,F., Scharmann,K., Eggers,C., Böttcher,B., Sokołowski,M., Shvetsova,E., Sharma,P., Roth,J., Rashiti,L., Glatt,S., et al. (2023) Ncs2* mediates in vivo virulence of pathogenic yeast through sulphur modification of cytoplasmic transfer RNA. Nucleic Acids Res., 51, 8133–8149.
- Glatt, S., Letoquart, J., Faux, C., Taylor, N.M.I., Seraphin, B. and Muller, C.W. (2012) The elongator subcomplex Elp456 is a hexameric RecA-like ATPase. *Nat. Struct. Mol. Biol.*, 19, 314–320.
- 46. Krutyhołowa,R., Hammermeister,A., Zabel,R., Abdel-Fattah,W., Reinhardt-Tews,A., Helm,M., Stark,M.J.R., Breunig,K.D., Schaffrath,R. and Glatt,S. (2019) Kti12, a PSTK-like tRNA dependent ATPase essential for tRNA modification by Elongator. Nucleic Acids Res., 47, 4814–4830.
- 47. Lin, T.Y., Smigiel, R., Kuzniewska, B., Chmielewska, J.J., Kosińska, J., Biela, M., Biela, A., Kościelniak, A., Dobosz, D., Laczmanska, I., et al.

- (2022) Destabilization of mutated human PUS3 protein causes intellectual disability. *Hum. Mutat.*, **43**, 2063–2078.
- 48. Lin,T.-Y., Kleemann,L., Jeżowski,J., Dobosz,D., Rawski,M., Indyka,P., Ważny,G., Mehta,R., Chramiec-Głąbik,A., Koziej,Ł., et al. (2024) The molecular basis of tRNA selectivity by human pseudouridine synthase 3. Mol. Cell, 84, 2472–2489.
- Pedre,B., Talwar,D., Barayeu,U., Schilling,D., Luzarowski,M., Sokolowski,M., Glatt,S. and Dick,T.P. (2023) 3-Mercaptopyruvate sulfur transferase is a protein persulfidase. *Nat. Chem. Biol.*, 19, 507–517.
- Noma,A., Sakaguchi,Y. and Suzuki,T. (2009) Mechanistic characterization of the sulfur-relay system for eukaryotic 2-thiouridine biogenesis at tRNA wobble positions. *Nucleic Acids Res.*, 37, 1335–1352.
- 51. Jüdes, A., Bruch, A., Klassen, R., Helm, M. and Schaffrath, R. (2016) Sulfur transfer and activation by ubiquitin-like modifier system Uba4•Urm1 link protein urmylation and tRNA thiolation in yeast. *Microb. Cell*, 3, 554–564.
- 52. Jüdes, A., Bruch, A., Klassen, R., Helm, M. and Schaffrath, R. (2016) Sulfur transfer and activation by ubiquitin-like modifier system Uba4•Urm1 link protein urmylation and tRNA thiolation in yeast. *Microb. Cell*, 3, 554–564.
- 53. Leimkühler,S., Wuebbens,M.M. and Rajagopalan,K.V. (2001) Characterization of *Escherichia coli* MoeB and its involvement in the activation of molybdopterin synthase for the biosynthesis of the molybdenum cofactor. *J. Biol. Chem.*, 276, 34695–34701.
- 54. Cairo, L.V., Hong, X., Müller, M.B.D., Yuste-Checa, P., Jagadeesan, C., Bracher, A., Park, S.-H., Hayer-Hartl, M. and Hartl, F.U. (2024) Stress-dependent condensate formation regulated by the ubiquitin-related modifier Urm1. Cell, 187, 4656–4673.
- Lake, M.W., Wuebbens, M.M., Rajagopalan, K.V. and Schindelin, H. (2001) Mechanism of ubiquitin activation revealed by the structure of a bacterial MoeB-MoaD complex. *Nature*, 414, 325–329.
- Lehmann, C., Begley, T.P. and Ealick, S.E. (2006) Structure of the Escherichia coli This-ThiF complex, a key component of the sulfur transfer system in thiamin biosynthesis. *Biochemstry*, 45, 11–19.
- Liu, Y., Vinyard, D. J., Reesbeck, M. E., Suzuki, T., Manakongtreecheep, K., Holland, P. L., Brudvig, G. W. and Söll, D. (2016) A [3Fe-4S] cluster is required for tRNA thiolation in archaea and eukaryotes. *Proc. Natl Acad. Sci. U.S.A.*, 113, 12703–12708.
- 58. Bimai,O., Legrand,P., Ravanat,J.-L., Touati,N., Zhou,J., He,N., Lénon,M., Barras,F., Fontecave,M. and Golinelli-Pimpaneau,B. (2023) The thiolation of uridine 34 in tRNA, which controls protein translation, depends on a [4Fe-4S] cluster in the archaeum methanococcus maripaludis. Sci. Rep., 13, 5351.